Journal of Translational Medicine

RESEARCH

Open Access

A novel peptide encoded by circSRCAP confers resistance to enzalutamide by inhibiting the ubiquitin-dependent degradation of AR-V7 in castration-resistant prostate cancer

Xiannan Meng[1†], Qingxuan Wu[4†], Chengsong Cao[5,6†], Wendong Yang[1], Sufang Chu[1], Hongjun Guo[7*], Suhua Qi[4*] and Jin Bai[1,2,3*]

Abstract

Background The sustained activation of androgen receptor splice variant-7 (AR-V7) is a key factor in the resistance of castration-resistant prostate cancer (CRPC) to second-generation anti-androgens such as enzalutamide (ENZ). The AR/AR-V7 protein is regulated by the E3 ubiquitin ligase STUB1 and a complex involving HSP70, but the precise mechanism remains unclear.

Methods High-throughput RNA sequencing was used to identify differentially expressed circular RNAs (circRNAs) in ENZ-resistant and control CRPC cells. The coding potential of circSRCAP was confirmed by polysome profiling and LC–MS. The function of circSRCAP was validated in vitro and in vivo using gain- and loss-of-function assays. Mechanistic insights were obtained through immunoprecipitation analyses.

Results A novel ENZ-resistant circRNA, circSRCAP, was identified and shown to be upregulated in ENZ-resistant C4-2B (ENZR-C4-2B) cells, correlating with increased AR-V7 protein levels. circSRCAP is generated via splicing by eIF4A3, forming a loop structure and is exported from the nucleus by the RNA helicase DDX39A. Mechanistically, circSRCAP encodes a 75-amino acid peptide (circSRCAP-75aa) that inhibits the ubiquitination of AR/AR-V7's co-chaperone protein HSP70 by disrupting the interaction with the E3 ligase STUB1. This process results in the upregulation of AR-V7 expression and promotes ENZ resistance in CRPC cells. Xenograft tumor models further confirmed the role of circSRCAP in CRPC progression and its potential as a therapeutic target for ENZ-resistant CRPC.

Conclusions circSRCAP provides an epigenetic mechanism influencing AR-V7 stability and offers a promising therapeutic target for treating ENZ-resistant CRPC.

Keywords Circular RNAs (circRNA), Castration-resistant prostate cancer (CRPC), AR-V7, Enzalutamide (ENZ)

†Xiannan Meng, Qingxuan Wu, and Chengsong Cao have contributed equally to this work.

*Correspondence:
Hongjun Guo
18966811618@163.com
Suhua Qi
suhuaqi@xzhmu.edu.cn
Jin Bai
bj@xzhmu.edu.cn
Full list of author information is available at the end of the article

Introduction

According to the latest data released in 2023, prostate cancer (PC) ranks as the malignant tumor with the highest estimated number of new cancer cases and the second highest in terms of deaths among men in the United States [1]. The androgen receptor (AR) signaling pathway plays a crucial role in the development and progression of PC [2–5]. Nearly all patients eventually develop androgen-independent castration-resistant prostate cancer (CRPC) during long-term androgen deprivation therapy (ADT) [6]. However, substantial evidence indicates that the malignant progression of CRPC still relies on increased androgen synthesis, overexpression of AR coactivators, AR amplification, and sustained AR activation [3, 5, 7–10]. These findings have spurred the development and clinical implementation of next-generation androgen receptor antagonists such as abiraterone acetate (ABI) and enzalutamide (ENZ). The utilization of ABI and ENZ has significantly improved the prognosis and quality of life of CRPC patients [11–16]. However, a substantial proportion of CRPC patients still develop resistance to ENZ within 1 year of treatment, leading to enzalutamide-resistant CRPC (ENZR-CRPC). This necessitates further investigation into the regulatory mechanisms of the AR axis.

AR genes have the capability to generate various AR splice variants (AR-Vs) through splicing mechanisms, thereby conferring resistance to ENZ [17–20]. Notably, the expression of AR-V7 escalates with the progression of CRPC and the development of ENZ resistance in patients [21–28]. AR-V7 arises from premature translation termination induced by AR gene rearrangement or aberrant mRNA splicing, resulting in a transcript characterized by the deletion of AR gene exons 4–8 and the incorporation of cryptic exon 3 (CE3) [18, 28–30]. The protein product encoded by AR-V7 lacks a ligand binding domain (LBD) and remains unresponsive to androgen receptor antagonists like Enz, thereby promoting the proliferation of PC cells [20, 28, 31]. These investigations affirm that AR-V7 potentially facilitates ligand-independent activation of the AR signaling pathway, culminating in resistance to endocrine therapies typified by Enz. Heat shock proteins (HSPs) modulate the activity and stability of numerous oncogenes pivotal for the survival and progression of cancer cells [32, 33]. The HSP70 family, encompassing stress-induced members HSP70 (HSPA1A/HSPA1B) and constitutively expressed member HSPC70 (HSPA8), assumes a crucial role in signal transduction and regulation of cancer cells by facilitating protein maturation and folding [34, 35]. STIP1 homology and U-box containing protein 1 (STUB1) function as a co-chaperone protein and functional E3 ubiquitin ligase, linking the peptide binding activity of HSP70 to the ubiquitin proteasome system. HSP70 interacts with STUB1 to regulate protein stability. Acting as a co-chaperone protein of AR and AR-V7, HSP70 forms a complex with STUB1, thereby modulating the stability of AR-V7 and participating in the drug resistance process of PC cells [36]. Nonetheless, there remains a significant gap in understanding the specific mechanisms underlying this effect.

Circular RNAs (circRNAs) represent a conserved and ancient class of non-coding RNAs characterized by covalently closed circular structures, closely linked to specific cellular functions and the pathogenesis of various diseases. Over the past decade, circRNAs have emerged as key players in tumorigenesis and disease progression, operating through diverse regulatory mechanisms [37–40]. Encoding functional peptides stands out as a significant mechanism through which circRNAs exert their biological effects. For instance, circTmeff1 facilitates muscle atrophy by interacting with TDP-43 and encoding a novel TMEFF1-339aa protein [41]. Another protein, circINSIG1-121, encoded by circINSIG1, modulates cholesterol metabolism by promoting the ubiquitin-dependent degradation of INSIG1, thereby contributing to the proliferation and metastasis of colorectal cancer [37]. Mechanistic investigations into circRNAs involved in prostate cancer development have also seen considerable advancement [42–45]. However, currently, no research has conclusively established the correlation between circRNA coding potential and the malignant progression of prostate cancer (PC) and castration-resistant prostate cancer (CRPC).

In this study, high-throughput sequencing was utilized to demonstrate that circSRCAP (circular RNA SRCAP, circBase ID: hsa_circ_0006127) exhibits significant overexpression in ENZ-resistant CRPC cells. Elevated circSRCAP expression enhances the stability of AR-V7, consequently promoting resistance to ENZ in CRPC cells. Notably, circSRCAP encodes a small peptide, circSRCAP-75aa (75aa), comprising 75 amino acids, which directly interacts with the HSP70 protein, thereby augmenting its stability. Furthermore, 75aa also impedes the association between HSP70 and STUB1, thus suppressing AR-V7 degradation through the ubiquitin–proteasome pathway. The expression of circSRCAP is modulated by the splicing factor eukaryotic translation initiation factor 4A3 (eIF4A3). It facilitates its nuclear export via DExD-box helicase 39A (DDX39A). Overall, our findings elucidate the role of circSRCAP, a circRNA implicated in drug resistance, as a pivotal regulatory element in AR-V7-driven CRPC

progression, offering a promising avenue for the treatment of ENZR-CRPC.

Materials and methods

Cell lines and cell cultures

The PC cell lines C4-2B, 22RV1, LNCaP, DU145, and PC-3 were cultured in RPMI1640 medium (Gibco, USA) supplemented with 10% fetal bovine serum (FBS, Gibco, USA). Human embryonic kidney 293T cells were maintained in DMEM supplemented with 10% FBS. All cell lines were obtained from the American Type Culture Collection (ATCC). The ENZ-resistant cell line ENZR-C4-2B was cultured in RPMI1640 complete medium containing 20 μM ENZ, which was acquired from MedChemExpress (MCE, USA). Cells were incubated in a humidified atmosphere at 37 °C with 5% CO_2.

Circular RNA sequencing

The samples utilized for circular RNA sequencing comprised the C4-2B and ENZR-C4-2B cell lines. Sequencing and subsequent analysis were carried out by Annoroad Gene Technology Corporation (Beijing, China). For circular RNA sequencing, total RNAs underwent treatment with a ribo-zero kit and RNase R to eliminate ribosomal RNA and linear RNA, respectively. Subsequently, a cDNA library was constructed, validated using an Agilent 2100 Bioanalyzer, and sequenced via Illumina RS-200-0048 platform. During the analysis, a criterion of log2 (|fold change|) ≥ 1.5 and p value <0.05 was employed to identify differentially expressed circRNAs. All relevant data have been deposited in the GEO database (Accession number: GSE264133). The detailed information of the sequencing data can be found in the GEO database (https://www.ncbi.nlm.nih.gov/geo/).

Reverse transcriptase PCR (RT-PCR) and quantitative real-time PCR (qRT-PCR)

Total RNA was isolated from C4-2B, ENZR-C4-2B, 22RV1, LNCaP, DU145, and PC-3 cell lines using Trizol (Yeasen, 19211ES60). The RNA was subsequently reverse-transcribed into cDNA and quantified via real-time PCR using ChamQ Universal SYBR qPCR Master Mix (Vazyme Biotech Co., Ltd, Nanjing, China). Relative expression levels of target genes were determined using the $2^{-\Delta\Delta Ct}$ method. All primers were synthesized by GENEWIZ Biological Technology (GENEWIZ, China), and their sequences are provided in Table S1.

Plasmid transfection and stable transfection

To construct the circSRCAP expression vector, the sequence of circSRCAP was amplified from 293T cDNA and inserted into the circular RNA expression plasmid PLO5-ciR (Geneseed, China). The circSRCAP-flag plasmid was generated by inserting the flag sequence immediately upstream of the stop codon of the putative ORF of circSRCAP. Additionally, to create a circSRCAP vector containing flanking intron sequences, the genomic region of circSRCAP along with its flanking introns was synthesized by Shanghai Genechem (Genechem, China) and cloned into the pCDNA3.1 vector. The full lengths of HA-Ubiquitin, Flag-circSRCAP, ATG mutation in the ORF of circSRCAP (Flag-Mut), circSRCAP ORF fused with Flag tag (Flag-75aa), SRCAP, HA-HSP70, truncated HSP70, HA-STUB1, and eIF4A3 were amplified from HEK293T cDNA using 2× TransStart® FastPfu PCR SuperMix (TransGen Biotech, AS221) and cloned into the pCDNA3.1 vector. For assessing the IRES activity of circSRCAP, the promoter region of firefly luciferase (F-Luc) in the psiCHECK2 vector was deleted, and the IRES sequences of circSRCAP were inserted downstream of Renilla luciferase (R-Luc). All plasmids were purified using an endotoxin-free plasmid extraction kit (Shandong Sparkjade Biotechnology Co., Ltd., AD0105). The construction of sh-circSRCAP, sh-HSP70, sh-eIF4A3, and sh-DDX39A involved cloning the respective shRNA sequences into the pLKO.1 vector. All shRNAs were obtained from Shanghai Genechem. The sequences of shRNAs are provided in Table S2. For stable transfection, 293T cells were transfected with the aforementioned vectors along with psPAX2 and pMD2G (Addgene) using jetPRIME® Transfection Reagent (Polyplus, USA) according to the manufacturer's instructions.

Antibodies

Anti-AR-V7 (Cell Signaling Technology, #19672), anti-HA (Proteintech, 81290-1-RR), anti-Flag (Proteintech, 80010-1-RR), anti-75aa (Abclonal, 1:1000), anti-HSP70 (Abcam, ab2787), anti-GST (Proteintech, 66001-2-Ig), anti-His (Proteintech, 66005-1-Ig), anti-STUB1 (Cell Signaling Technology, #2080), anti-eIF4A3 (Proteintech, 17504-1-AP), anti-DDX39A (Proteintech, 11723-1-AP), anti-ubiquitin (Ub, Proteintech, 10201-2-AP) and anti-Tubulin (Proteintech, 66031-1-Ig).

Actinomycin D assay

For the Actinomycin D assay, total RNAs extracted were treated with 1 μg/mL actinomycin D (Sigma-Aldrich, USA) to inhibit new RNA synthesis for 0, 2, 4, 8, 12, and 24 h, respectively.

Nucleocytoplasmic separation

The RNA from nuclear and cytoplasmic fractions of ENZR-C4-2B or 22RV1 cells was extracted using a Paris kit (Invitrogen, USA) following the manufacturer's instructions.

Cell growth and survival assay

ENZR-C4-2B or C4-2B cells were seeded onto 12-well plates at a density of 0.5×10^5 cells per well in RPMI 1640 media supplemented with 10% FBS. Subsequently, they were transfected with the corresponding plasmids and treated with 20 μM ENZ in media containing FBS. Total cell numbers were enumerated after 3 and 6 days.

In cell survival assay, ENZR-C4-2B or C4-2B cells were seeded onto 12-well plates at a density of 0.3×10^5 cells per well in RPMI 1640 media supplemented with 10% FBS. Following transfection with the respective plasmids, cells were treated with varying concentrations of ENZ (0, 10, 20, 40, and 80 μM) for 3 days. Total cell numbers were assessed at the end of the 3-day period.

Western blot

Total protein was isolated from the cells following various treatments. Briefly, cells were washed three times with PBS and lysed in an ice-cold extraction buffer (50 mM Tris–HCl pH 7.4, 150 mM NaCl, 1% NP, 0.1% SDS, and 1× protease inhibitor cocktail). Protein concentration was determined by the Bradford method. Proteins were separated using sodium dodecyl sulfate–polyacrylamide gel electrophoresis (SDS-PAGE) and electroblotted onto a polyvinylidene fluoride (PVDF) membrane (Roche, Basel, Switzerland) by standard procedures. Transferred blots were incubated sequentially with anti-AR-V7, anti-HA, anti-Flag, anti-75aa, anti-HSP70, anti-GST, anti-His, anti-STUB1, anti-eIF4A3, anti-DDX39A, anti-ubiquitin or anti-Tubulin at 4 °C for 12 h, and HRP-conjugated secondary antibodies. Protein bands were visualized with an enhanced chemiluminescence detection kit and recorded on a radiographic film (Alpha Innotech, San Jose, CA, USA).

Co-immunoprecipitation (Co-IP)

Cells were lysed using Western blot and immunoprecipitation (IP) lysis buffer (Beyotime, China) supplemented with protease inhibitor (MCE, USA). After centrifugation, the supernatant was collected and incubated with primary antibody at 4 °C overnight. Subsequently, the lysate was incubated with 30 μL of protein A/G magnetic beads (MCE) at room temperature for 4 h. The collected beads-protein was washed six times and then subjected to analysis in subsequent experiments.

Cycloheximide (CHX) chase assay

Cells in each experimental group were treated with 10 μg/mL CHX (MCE) for various durations: 0, 1, 2, 4, and 8 h. The expression levels of proteins were assessed using Western blot analysis.

Ubiquitination assay

Cells subjected to different treatments were treated with 5 μM MG132 (MCE) for 6 h. Subsequently, cell lysates were prepared using PierceTM IP lysis buffer (Thermo Fisher Scientific, USA) supplemented with a protease inhibitor cocktail (Thermo Fisher Scientific, USA). The lysates were then incubated with specific antibodies and Protein A/G beads overnight at 4 °C. Finally, the protein A/G beads containing the bound immunoprecipitates were collected and analyzed using Western blotting.

Immunofluorescence assay

For the immunofluorescence assay, cells were harvested using ice-cold PBS. Subsequently, the cells were fixed with 4% paraformaldehyde for 30 min at room temperature, followed by treatment with 0.2% Triton X-100 for 10 min. Afterward, the cells were incubated with 10% goat serum for 60 min at 37 °C and then exposed to primary antibodies at 4 °C overnight. Following PBS washing, the cells were incubated with corresponding fluorescent secondary antibodies and counterstained for nuclei using 4′,6-diamidino-2-phenylindole (DAPI) (Solarbio, China) for 15 min at room temperature.

Fluorescence in situ hybridization (FISH) assay

According to the manufacturer's instructions, the FISH kit (Ribo Bio, Guangzhou, China) was employed to conduct FISH in cells, and the results were visualized using a confocal laser-scanning microscope (LSM 880, Carl Zeiss Jena, Jena, Germany). Cells were fixed with 4% paraformaldehyde at room temperature for 10 min, followed by treatment with 0.5% Triton X-100 in phosphate-buffered saline (PBS) at 4 °C for 5 min. Subsequently, the cells were pre-hybridized using Pre-hybridization Buffer at 37 °C for 30 min. Finally, the cells were subjected to hybridization with 2.5 μL of 20 μM circSRCAP FISH probes (Ribo Bio, Guangzhou, China) overnight at 37 °C. The probe sequences are provided in Table S3.

Polysome profiling analysis

293T cells were seeded in 15 cm plates and transfected with either circSRCAP plasmid or Flag-Mut plasmid. After 48 h, the cells were treated with 100 μg/mL CHX in DMSO for 5 min at 37 °C. They were then washed twice with ice-cold PBS and harvested by trypsinization for polysome profiling. Cell lysis was performed in 500 μL of polysome lysis buffer [5 mM Tris–HCl (pH 7.5), 2.5 mM $MgCl_2$, 1.5 mM KCl, 1× protease inhibitor cocktail (EDTA-free), 0.5% Triton X-100, 2 mM DTT, 0.5% sodium deoxycholate, 100 units RNase inhibitor, and 100 μg/mL CHX] on ice for 15 min, followed by centrifugation at 4 °C for 7 min at 16,000×*g* to pellet nuclei and mitochondria. The supernatant was then loaded onto

a 5–50% (w/v) sucrose density gradient and ultracentrifuged at 20,000×*g* for 2 h at 4 °C using a Beckman SW41 rotor, followed by fractionation using a BioComp PGFip Piston Gradient Fractionator Model 152. Absorbance at 254 nm was measured using an absorbance detector connected to the fraction collector. RNA was extracted from fractions using TriZol LS solution, and qRT-PCR was conducted to evaluate the levels of circSRCAP and SRCAP mRNA in the indicated fractions.

Liquid chromatography-tandem mass spectrometry (LC–MS)

Proteins were separated via SDS-PAGE and subsequently subjected to digestion using sequencing-grade trypsin (Promega, Madison, WI, USA). The resulting digested peptides were analyzed using a QExactive mass spectrometer (Thermo Fisher Scientific, Waltham, MA, USA). Fragment spectra were then analyzed utilizing the National Center for Biotechnology Information nonredundant protein database with Mascot software (Matrix Science, Boston, MA, USA).

GST pull-down assay

The plasmids encoding GST-HSP70$^{\Delta 291-641}$ and His-75aa were transfected into *E. coli*. For cell lysis, cells were lysed on ice in lysis buffer (50 mM Tris–HCl, pH 7.5, 150 mM NaCl, 1% NP-40, 1 mM EDTA) supplemented with a complete protease inhibitor cocktail for 30 min. The lysate was clarified by centrifugation at 12,000×*g* for 15 min at 4 °C. Clarified lysate was mixed with 100–200 µL of pre-washed GST beads and incubated for 1–2 h at 4 °C with gentle rotation. After three washes with wash buffer (50 mM Tris–HCl, pH 7.5, 150 mM NaCl, 0.1% NP-40), the target protein was diluted to 1–2 mg/mL in lysis buffer (1:10 ratio) and added to the GST beads, incubating overnight at 4 °C. The beads were washed three times with wash buffer for 5–10 min each, followed by elution of bound proteins using 10–20 mM reduced glutathione in lysis buffer for 10–30 min at room temperature. Finally, eluted proteins were subjected to SDS-PAGE followed by Western blot to analyze protein interactions.

RIP (RNA Immunoprecipitation) assays

The RIP assay was performed using the PureBinding® RNA Immunoprecipitation Kit (GENESEED, P0101), following the manufacturer's instructions. In brief, protein A/G magnetic beads were incubated with the primary antibody or IgG (MCE, USA) separately, and then incubated with cells. Subsequently, RNA was co-precipitated and extracted, and finally quantitated using qRT-PCR. The primer sequences are listed in Table S4.

Biotin RNA pull-down assay

Cells were lysed by ultrasonication in RIP buffer (150 mM KCl, 25 mM Tris–HCl, pH 7.4, 0.5 mM dithiothreitol, 0.5% NP-40) supplemented with protease inhibitors and RNase inhibitors. The cell lysates were then precleared with streptavidin magnetic beads (MCE, USA). In vitro transcribed biotin-labeled RNA or DNA probes adsorbed to streptavidin magnetic beads were subsequently incubated with cell lysates at 4 °C for 6 h before washing three times with RIP buffer. Finally, the potential interacting proteins were evaluated using Western blot analysis.

MS2-RIP assay

MS2-RIP assays were conducted following the instructions provided with the Millipore Magna RIP Kit (Millipore, Darmstadt, Germany). The 6× MS2 stem loop was fused to the circSRCAP plasmid. Cells of interest were co-transfected with the target RNA expression vector fused with the MS2 stem loop and the MS2-GFP vector. Subsequently, these cells were lysed using RIP lysis buffer containing protease and RNase inhibitors. After centrifugation to clear the cell lysate, the supernatant was incubated with anti-GFP/IgG antibody-conjugated beads overnight at 4 °C. Following thorough washing, the binding complexes were eluted, purified, and analyzed by qRT-PCR or Western blot.

Animal experiments

For the xenograft model, fifteen 6-week-old male BALB/c nude mice were randomly assigned to three groups. After 1 week of acclimatization, 1×10^7 ENZR-C4-2B cells (scramble, sh-circSRCAP #1, or sh-circSRCAP #2) were combined with matrix gel in a 1:1 ratio and injected subcutaneously into the dorsal region of the mice. Once the tumor volume reached approximately 50 mm^3, ENZ (25 mg/kg, administered orally) was administered. Tumor volume was monitored every 7 days. After 6 weeks of treatment, tumor tissues were collected and subjected to immunohistochemical (IHC) staining.

IHC

Paraffin sections were initially deparaffinized and rehydrated. Antigen retrieval was performed, and endogenous peroxidase activities were blocked. Subsequently, the sections were incubated overnight at 4 °C with the specified antibodies. Following this, the sections were incubated with a horseradish peroxidase-conjugated secondary antibody and subjected to DAB (3,3′-diaminobenzidine) staining. Finally, counterstaining was performed using hematoxylin.

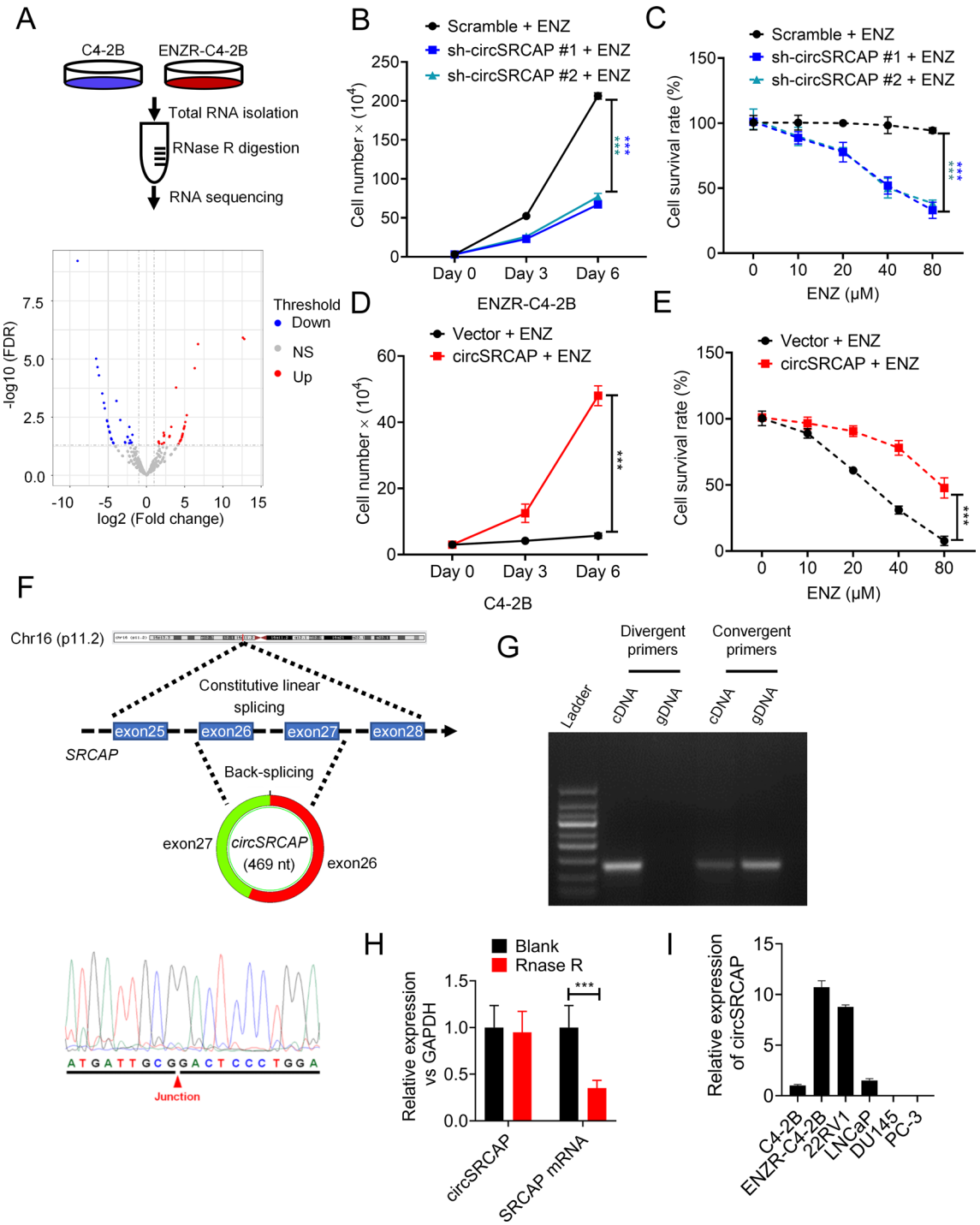

Fig. 1 circSRCAP exhibits high expression levels in CRPC cells. **A** Differentially expressed circRNAs in ENZR-C4-2B and C4-2B cells, analyzed by circRNA-seq and visualized using volcano plots. **B** Total cell count in ENZR-C4-2B cells transfected with shRNAs targeting scramble or circSRCAP, after treatment with 10 μM ENZ for 0, 3, and 6 days. **C** Cell count in ENZR-C4-2B cells transfected with shRNAs targeting scramble or circSRCAP, followed by treatment with various ENZ concentrations for 3 days. **D** Total cell count in C4-2B cells transfected with vector or circSRCAP overexpression plasmids, after 10 μM ENZ treatment for 0, 3, and 6 days. **E** Cell count in C4-2B cells transfected with vector or circSRCAP plasmids, followed by treatment with different ENZ concentrations for 3 days. **F** Genomic locus of circSRCAP and SRCAP gene, with Sanger sequencing confirming reverse splicing of SRCAP exons 26 and 27 (red arrows). **G** PCR detection of circSRCAP expression in cDNA and genomic DNA from ENZR-C4-2B cells using convergent/divergent primers. **H** Stability of circSRCAP and linear SRCAP mRNA analyzed by qRT-PCR with/without RNase R treatment. **I** qRT-PCR analysis of circSRCAP expression in various cell lines, including C4-2B, ENZR-C4-2B, 22RV1, LNCaP, DU145, and PC-3. Values are mean ± SD. Statistical significance was determined by one-way ANOVA (*** $p < 0.001$)

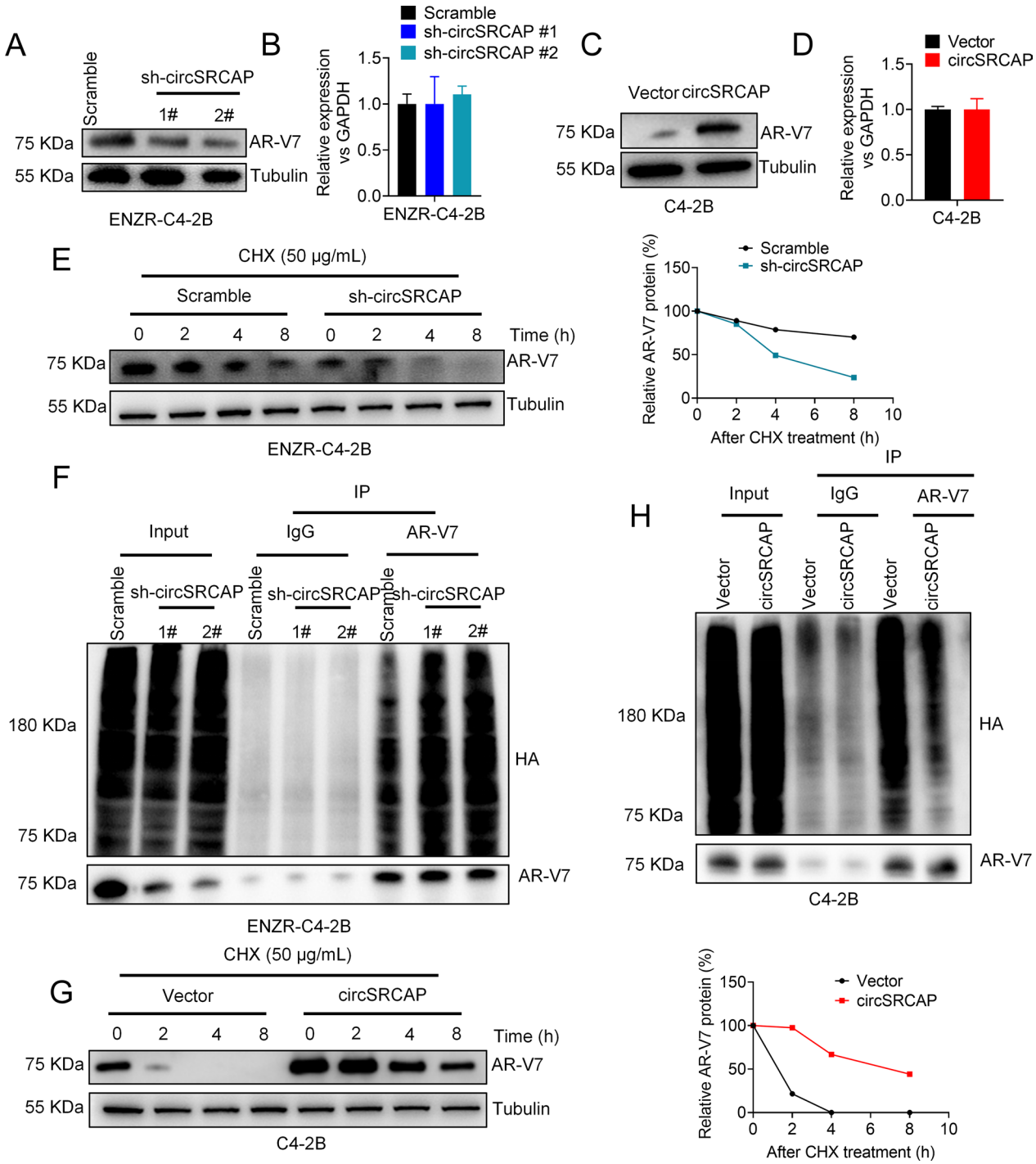

Fig. 2 Highly expressed circSRCAP increases the expression of AR-V7 protein in ENZR-C4-2B. **A** Western blot analysis of AR-V7 protein expression in ENZR-C4-2B cells transfected with scramble or circSRCAP shRNAs. **B** qRT-PCR analysis of AR-V7 mRNA expression in ENZR-C4-2B cells transfected with scramble or circSRCAP shRNAs. **C** Western blot detection of AR-V7 protein in C4-2B cells transfected with vector or circSRCAP overexpression plasmids. **D** qRT-PCR analysis of AR-V7 mRNA expression in C4-2B cells transfected with vector or circSRCAP overexpression plasmids. **E** ENZR-C4-2B cells transfected with scramble or circSRCAP shRNA were treated with 50 μg/mL cycloheximide (CHX), and AR-V7 half-life was assessed by Western blot at 0, 2, 4, and 8 h. **F** ENZR-C4-2B cells transfected with HA-ubiquitin (HA-Ub) and treated with scramble or circSRCAP shRNA for 48 h, followed by 5 μM MG132 for 6 h. Immunoprecipitation with AR-V7 antibody was followed by Western blot. **G** C4-2B cells transfected with vector or circSRCAP overexpression plasmids were treated with 50 μg/mL CHX, and AR-V7 half-life was assessed by Western blot at 0, 2, 4, and 8 h. **H** C4-2B cells transfected with HA-Ub and treated with vector or circSRCAP overexpression plasmids for 48 h, followed by 5 μM MG132 for 6 h. Immunoprecipitation with AR-V7 antibody and Western blot

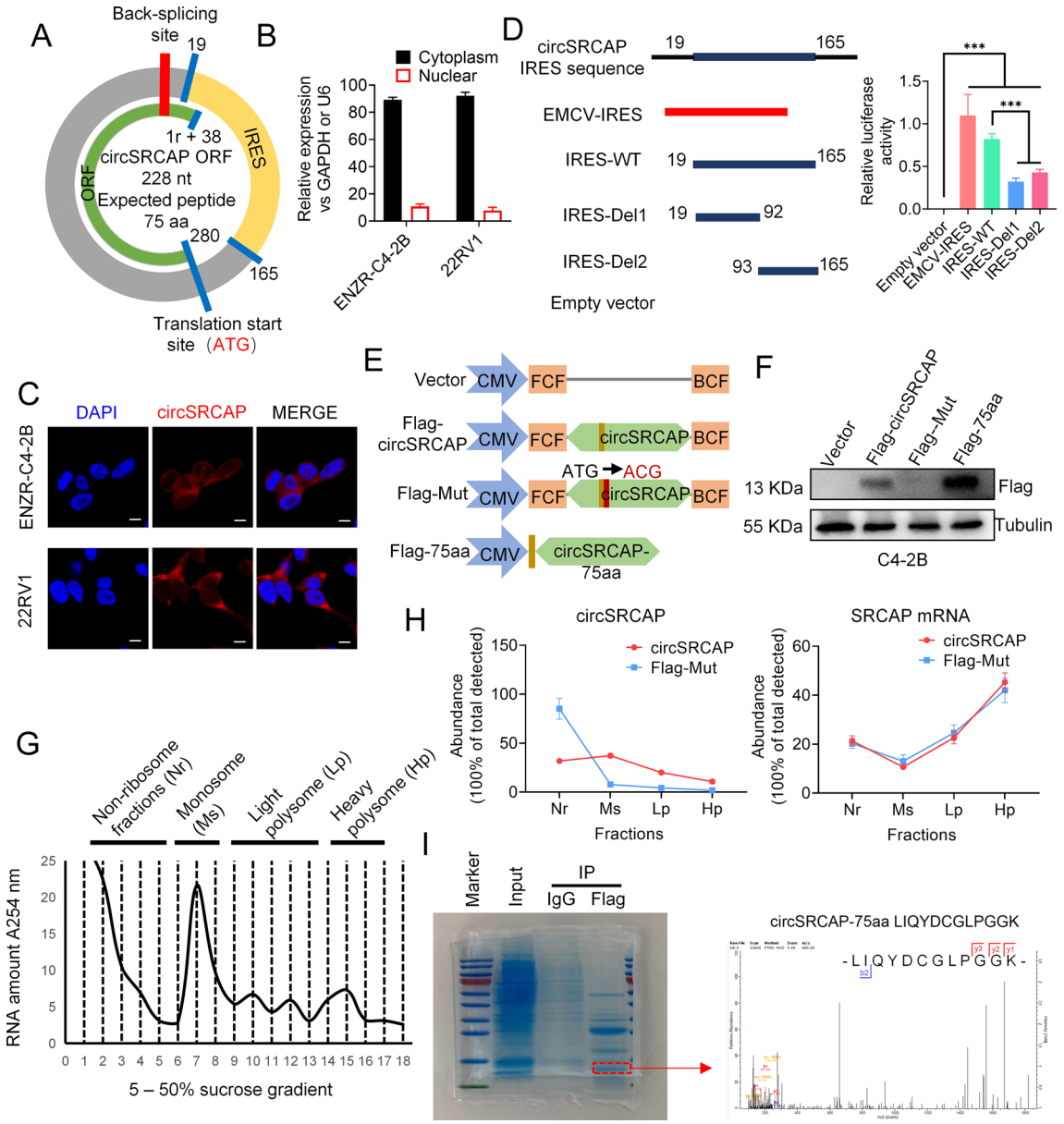

Fig. 3 circSRCAP encodes a novel small peptide circSRCAP-75aa (75aa). **A** Diagram illustrating the open reading frame (ORF) of circSRCAP, including start/stop codons and the internal ribosome binding sequence (IRES). **B** Distribution of circSRCAP in the nucleus and cytoplasm analyzed by qRT-PCR, with U6 and GAPDH as nuclear and cytoplasmic markers, respectively. **C** Fluorescence in situ hybridization (FISH) images of circSRCAP in ENZR-C4-2B and 22RV1 cells. Scale bar = 10 μm. **D** Luciferase reporter assays in 293T cells transfected with full-length IRES and truncated fragments of circSRCAP to assess Luc/Rluc activity ($n = 6$ per group). **E** Cloning of Flag-tagged circSRCAP, Flag-circSRCAP, ATG mutant (Flag-Mut), and Flag-75aa ORF constructs into CMV expression vectors for Western blot detection of the 75aa peptide. **F** Western blot analysis of Flag-tag expression in 293T cells transfected with vector, Flag-circSRCAP, Flag-Mut, or Flag-75aa. **G** Polysome profiling in 293T cells transfected with circSRCAP or Flag-Mut plasmids, followed by separation of cell lysates using a 5–50% sucrose gradient. **H** qRT-PCR analysis of circSRCAP and SRCAP mRNA in polysome profiling fractions (Nr, Ms, Lp, Hp) from G. **I** LC–MS detection of the 75aa peptide expression in 293T cells overexpressing circSRCAP

Statistical analysis

GraphPad Prism Software (GraphPad Software, La Jolla, CA, USA) was used to perform statistical analysis. Two-tailed *t* Student's test and one-way ANOVA analysis were performed for statistical comparisons. All statistics analysis data were expressed as mean ± standard error of the mean. A p value <0.05 was considered statistically significant.

Results

circSRCAP promotes resistance of CRPC cells to ENZ by upregulating the expression of AR-V7.

In this study, C4-2B cells were cultured in complete medium containing increasing concentrations of ENZ over a period of more than 12 months, resulting in the development of ENZR-C4-2B cells [46]. RNA-Seq analysis identified 147 differentially expressed circRNAs between C4-2B and ENZR-C4-2B cells (Fig. 1A; Additional file 1). Generally, higher expression levels of RNA transcripts in cells correlate with stronger regulatory effects on cellular functions. In the case of ENZR-C4-2B cells, we conducted an analysis of the transcript expression levels of significantly upregulated circRNAs. Further analysis revealed that among the top ten circRNAs in ENZR-C4-2B cells, six were derived from coding genes. Knockdown experiments were performed on these six circRNAs (circASPH, circFCHO2, circFASN, circSRCAP, circPPIB, circTMPRSS2) using shRNAs in ENZR-C4-2B cells cultured in complete medium containing ENZ. Notably, knockdown of circSRCAP significantly inhibited cell proliferation, whereas knockdown of SRCAP mRNA did not have the same effect (Fig. 1B, C; Fig. S1A–F). Conversely, overexpression of circSRCAP in C4-2B cells significantly increased resistance to ENZ, while overexpression of SRCAP mRNA did not produce a similar effect (Fig. 1D, E; Fig. S1G). These findings indicate that circSRCAP may play a role in reducing the resistance of ENZR-C4-2B cells to ENZ. Sanger sequencing confirmed that circSRCAP was generated by reverse splicing of the 26th and 27th exons of the SRCAP gene, forming a circular RNA molecule with a unique sequence distinct from SRCAP mRNA (Fig. 1F). PCR analysis using cDNA and genomic DNA (gDNA) templates showed that circSRCAP could only be amplified with divergent primers from cDNA templates, while both cDNA and gDNA templates yielded amplification with convergent primers, indicating the specific reverse splicing pattern of circSRCAP (Fig. 1G). Additionally, the half-life of circSRCAP was found to be longer compared to SRCAP mRNA, as demonstrated by the Actinomycin D assay (Fig. S1H, I). Furthermore, RNase R treatment of total RNA from ENZR-C4-2B cells showed that the stability of circSRCAP was significantly higher than that of SRCAP mRNA (Fig. 1H). Overall, these results suggest that circSRCAP exists predominantly in a circular form and may contribute to the resistance of ENZR-C4-2B cells to ENZ.

The AR-V7 protein stands out as the most crucial mechanism known for safeguarding CRPC cells against ENZ. Notably, circSRCAP exhibits predominant expression in AR-V7-positive cells (ENZR-C4-2B and 22RV1), weakly positive cells (C4-2B and LNCaP), but not in AR-V7-negative cells (DU145 and PC-3) (Fig. 1I). Through experiments involving overexpression and knockdown of circSRCAP in C4-2B and ENZR-C4-2B cells, respectively, it was observed that reduced circSRCAP expression inhibited AR-V7 protein levels in ENZR-C4-2B cells without affecting its mRNA levels (Fig. 2A, B). Conversely, elevated circSRCAP expression promoted AR-V7 protein levels in C4-2B cells without affecting mRNA levels (Fig. 2C, D). Further investigations in this study have demonstrated that alterations in circSRCAP expression, whether decreased or increased, can respectively diminish or augment the stability of the AR-V7 protein, thereby modulating its ubiquitination-mediated degradation (Fig. 2E–H). In summary, circSRCAP exhibits the capability to elevate AR-V7 protein expression, thus potentially serving as a key regulatory factor contributing to drug resistance in CRPC.

The novel small peptide circSRCAP-75aa (75aa) is encoded by circSRCAP

circRNAs are primarily recognized for their involvement in post-transcriptional regulation. Emerging evidence suggests that some circRNAs have the capability to encode functional peptides [47, 48]. In the case of circSRCAP, it contains an internal ribosome entry site (IRES) sequence and an open reading frame (ORF) spanning 228 nucleotides across the back-splicing site. Notably, these elements are predominantly localized in the cytoplasm of ENZR-C4-2B cells and 22RV1 cells (Fig. 3A–C). To validate the translation initiation potential of the IRES sequence, a dual luciferase reporter gene experiment was conducted. Results revealed higher F-Luc/R-Luc activity

(See figure on next page.)

Fig. 4 75aa enhances the resistance of CRPC to ENZ both in vivo and in vitro. **A** Total cell count in C4-2B cells transfected with vector, Flag-circSRCAP, Flag-Mut, or Flag-75aa plasmids, after treatment with 10 μM ENZ for 0, 3, and 6 days. **B** Total cell count in C4-2B cells transfected with vector, Flag-circSRCAP, Flag-Mut, or Flag-75aa plasmids, followed by treatment with various ENZ concentrations for 3 days. **C** Western blot detection of AR-V7 protein expression in C4-2B cells transfected with vector, Flag-circSRCAP, Flag-Mut, or Flag-75aa plasmids. **D** AR-V7 half-life in C4-2B cells transfected with vector, Flag-circSRCAP, Flag-Mut, or Flag-75aa plasmids, followed by treatment with 50 μg/mL cycloheximide (CHX) and Western blot analysis at 0, 2, 4, and 8 h. **E** Immunoprecipitation with AR-V7 antibody and Western blot analysis in C4-2B cells transfected with HA-Ub and vector, Flag-circSRCAP, Flag-Mut, or Flag-75aa plasmids, followed by treatment with 5 μM MG132 for 6 h. **F**–**H** BALB/c nude mice ($n = 5$ per group) were subcutaneously injected with ENZR-C4-2B cells stably transfected with scramble or circSRCAP shRNA. Tumor weight and volume were measured. Statistical significance was determined by one-way ANOVA (** $p < 0.01$, *** $p < 0.001$)

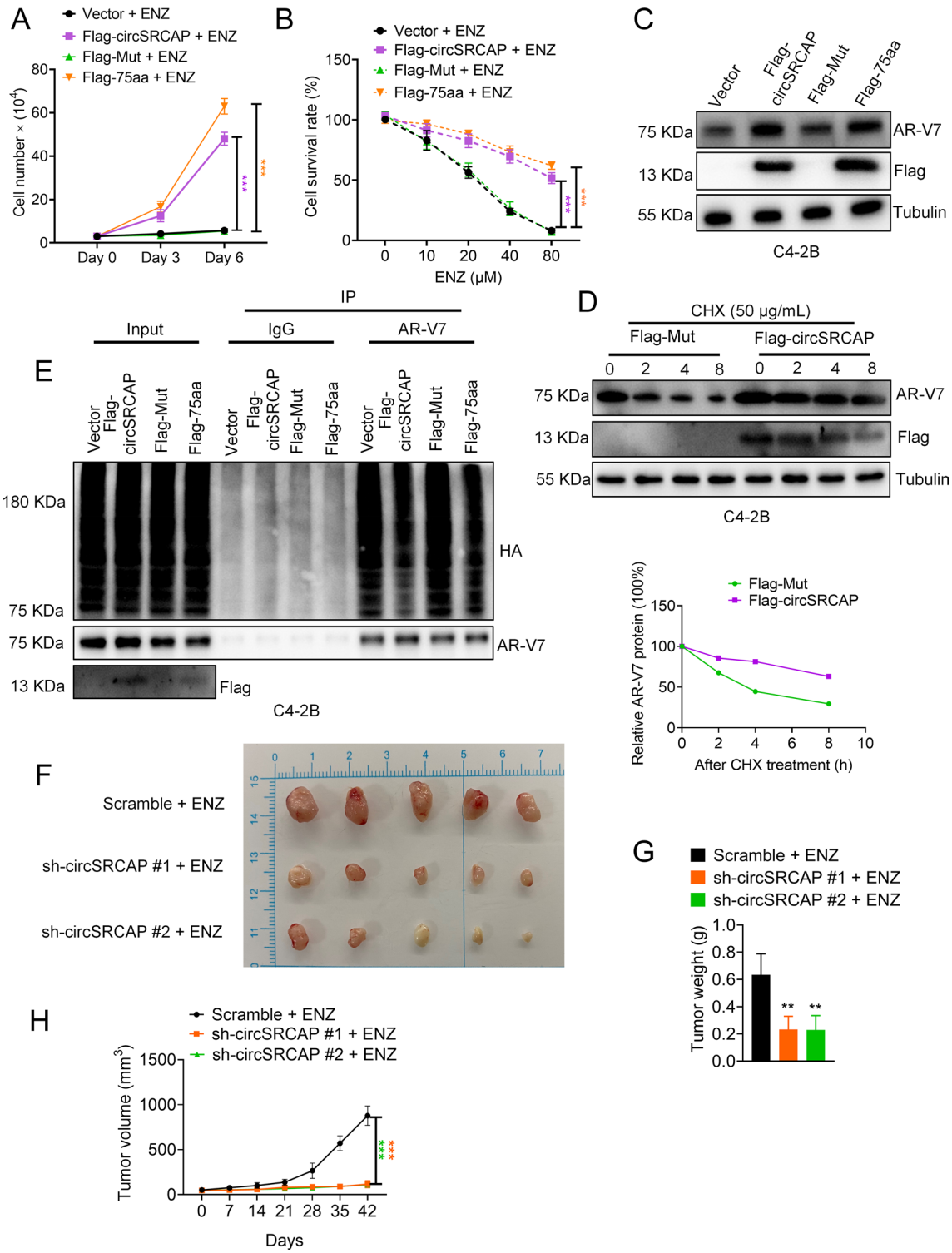

Fig. 4 (See legend on previous page.)

with the IRES sequence compared to empty vectors and truncated IRESs (Fig. 3D). This suggests that the IRES-driven ORF may encode a small peptide, circSRCAP-75aa, consisting of 75 amino acids. To confirm the coding ability of circSRCAP, four plasmids were constructed: Vector, Flag-circSRCAP, Flag-Mut, and Flag-75aa, and transfected into 293T cells (Fig. 3E). Subsequent analysis demonstrated that transfection with Flag-cicSRCAP and

Flag-75aa resulted in the production of a small peptide approximately 13 kDa in size (Fig. 3F). Polysome profiling via sucrose density gradient centrifugation further supported the translation of circSRCAP. 293T cells transfected with circSRCAP and Flag-Mut vectors were subjected to sucrose gradient centrifugation, which revealed circSRCAP predominantly in all polymeric fractions. Conversely, after ATG mutation, circSRCAP was mainly enriched in the non-ribosome component, without affecting the distribution of SRCAP mRNA, indicating active translation of circSRCAP (Fig. 3G, H). Moreover, overexpression of circSRCAP in 293T cells facilitated the identification of the specific amino acid sequence (LIQYDCGLPGGK) of the 75-amino acid peptide through LC–MS (Fig. 3I). These findings collectively demonstrate that circSRCAP can be translated into a novel 75-amino acid peptide in an IRES-dependent manner.

75aa promote CRPC cell resistance to ENZ by inhibiting AR-V7 degradation in vitro and in vivo

Overexpression of circSRCAP and 75aa in C4-2B cells enhances their resistance to ENZ and inhibits AR-V7 degradation via the ubiquitin–proteasome pathway (Fig. 4A–E). To investigate the in vivo role of circSRCAP in CRPC resistance to ENZ, we employed a subcutaneous xenograft model. The findings revealed that knockdown of circSRCAP in ENZR-C4-2B cells significantly increased tumor sensitivity to ENZ (Fig. 4F–H). After preparing a specific antibody for 75aa and confirming its specificity through LC–MS, we assessed the expression of Ki67, AR-V7, and 75aa in tumor tissues (Fig. S2A). The results indicated that knockdown of circSRCAP notably reduced the protein level of 75aa and suppressed the protein expression of Ki67 and AR-V7 in tumor tissues (Fig. S2B). These results were consistent with those observed in vitro, while SRCAP mRNA knockdown did not affect tumor tissue tolerance to ENZ (Fig. S2C–E).

75aa interacts with HSP70, preventing its protein degradation and disrupting the formation of the HSP70-STUB1 complex.

To elucidate how 75aa influences the stability of AR-V7 protein, we transfected the Flag-circSRCAP plasmid into C4-2B cells and investigated the binding partners of 75aa through Co-IP coupled with LC–MS. Our analysis revealed that 75aa could specifically bind to HSP70 protein (Fig. 5A). HSP70 forms a specialized complex with AR-V7, facilitating its stability through interactions with STUB1. Reduced levels or inhibition of HSP70 result in AR-V7 degradation via the ubiquitin–proteasome pathway [36]. In 293T cells, co-transfection of mCherry-circSRCAP and HA-HSP70 plasmids followed by immunofluorescence showed predominant nuclear co-localization of the two proteins (Fig. 5B). Co-IP experiments in C4-2B cells demonstrated that exogenously expressed HSP70 could bind to 75aa, and endogenous HSP70 in ENZR-C4-2B cells exhibited a similar binding capacity to 75aa (Fig. 5C, D). HSP70 comprises two main domains: the nucleotide-binding domain (NBD) and the substrate-binding domain (SBD), with a disordered region (DR) located near the C-terminal end. We constructed various truncated plasmids based on the length of these domains: full-length HSP70 plasmid (HA-HSP70), NBD plasmid (HA-Δ1), NBD and SBD deletion plasmid (HA-Δ2), and SBD plasmid (HA-Δ3) (Fig. 5E). Co-IP experiments revealed that 75aa could interact with both full-length HSP70 and the truncated protein containing the DR region, whereas the deletion of the DR region abolished the binding of 75aa (Fig. 5F). This indicates that 75aa specifically binds to the DR region of HSP70. To investigate the direct interaction between 75aa and HSP70, we performed GST pull-down assays using His-75aa and GST-HSP70$^{\Delta 291-641}$ (including the DR region) in the *E. coli* system. SDS-PAGE and Western blot analysis confirmed that GST-HSP70$^{\Delta 291-641}$ directly interacts with 75aa, while GST alone did not exhibit such binding (Fig. 5G). These findings collectively suggest that circSRCAP interacts with HSP70 through the encoded 75aa.

Silencing circSRCAP in ENZR-C4-2B cells notably diminished the protein levels of HSP70 without affecting its mRNA expression (Fig. 6A; Fig. S3A). Similarly, overexpression of circSRCAP in C4-2B cells did not alter HSP70 mRNA levels but significantly increased its protein expression (Fig. 6B; Fig. S3B). This indicates that circSRCAP regulates HSP70 protein expression through 75aa coding (Fig. 6C). Diminished expression of 75aa in ENZR-C4-2B cells led to decreased HSP70

(See figure on next page.)

Fig. 5 75aa directly binds to HSP70. **A** LC–MS analysis identified HSP70 protein fragments bound to the 75aa peptide. **B** Immunofluorescence analysis of 293T cells co-transfected with mCherry-circSRCAP and HA-HSP70 plasmids, showing colocalization of 75aa and HSP70. Scale bar = 20 μm. **C** Immunoprecipitation of Flag-75aa and HA-HSP70 from total lysates of 293T cells, followed by Western blot detection. **D** Immunoprecipitation of 75aa or HSP70 antibodies from total lysates of ENZR-C4-2B cells, followed by Western blot detection. **E** Schematic diagram of the constructed plasmids. **F** Co-transfection of HSP70 mutant truncation and Flag-75aa plasmids in 293T cells, followed by immunoprecipitation with Flag or HA antibodies and Western blot analysis. **G** Detection of His-75aa and GST-HSP70$^{\Delta 291-641}$ proteins expressed in *E. coli* using a GST pull-down assay

A

Sequence	Length	Mass	Start position	End position	Gene names	Protein names	Score
DAGVIAGLNVLR	12	1196.7	137	148	HSPA1A	Heat shock 70 kDa protein 1A	73.23
FEELCSDLFR	10	1314.6	304	313	HSPA1A	Heat shock 70 kDa protein 1A	117.9
ITITNDK	7	803.44	476	482	HSPA1A	Heat shock 70 kDa protein 1A	121.3
LLQDFFNGR	9	1108.6	326	334	HSPA1A	Heat shock 70 kDa protein 1A	64.21
TTPSYVAFTDTER	13	1486.7	37	49	HSPA1A	Heat shock 70 kDa protein 1A	57.84

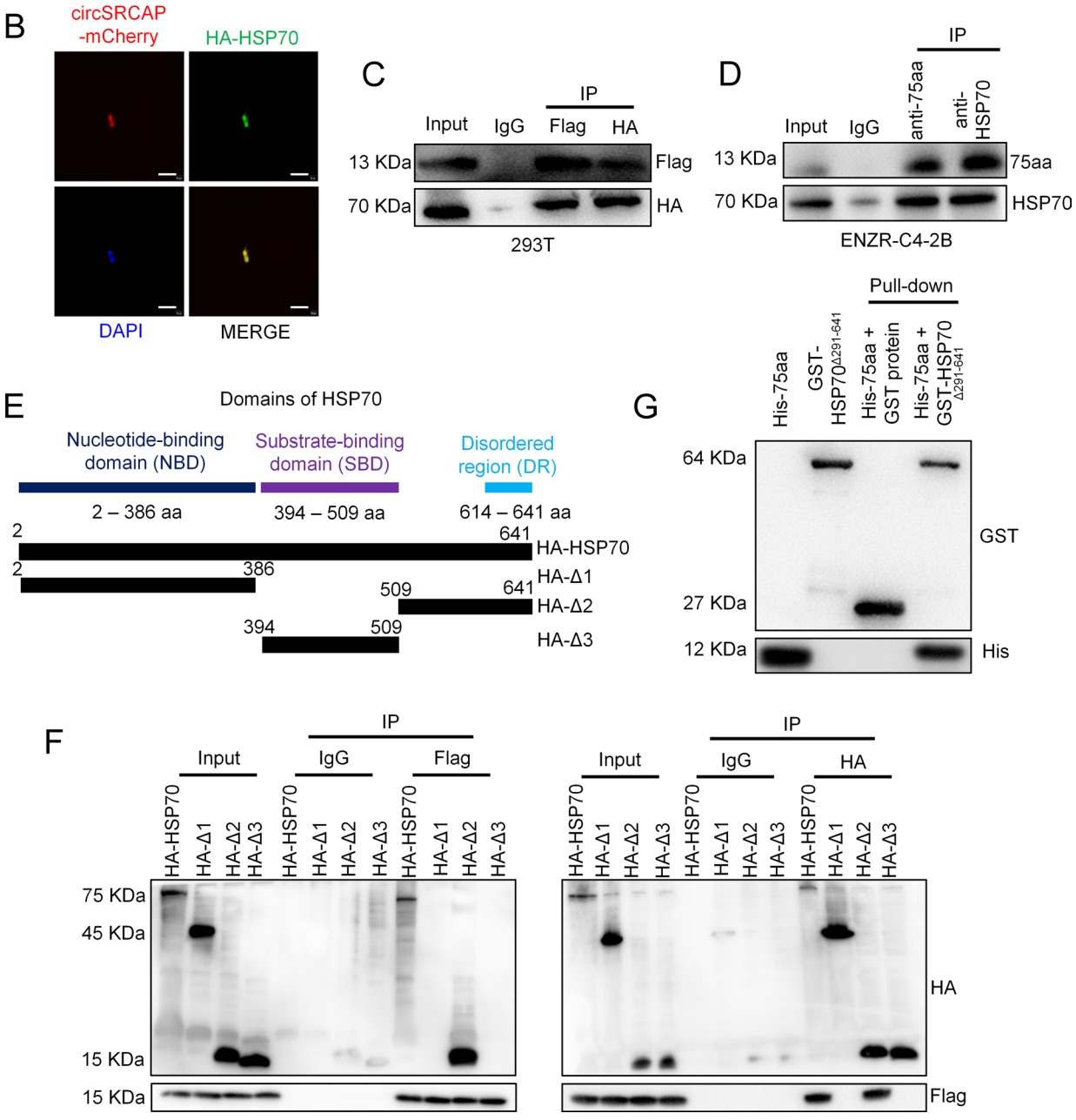

Fig. 5 (See legend on previous page.)

protein stability, promoted HSP70 degradation via the ubiquitin–proteasome pathway, and enhanced the interaction between HSP70 and STUB1 (Fig. 6D–F). Conversely, elevating 75aa expression in C4-2B cells enhanced HSP70 protein stability, inhibited HSP70 degradation through the ubiquitin–proteasome pathway, and reduced the binding of HSP70 to STUB1 (Fig. 6G–I). These findings confirm that 75aa enhances HSP70 protein stability and disrupts the HSP70-STUB1 complex.

75aa participates in the process of regulating AR-V7 expression by HSP70-STUB1 complex

Firstly, we transfected the HA-HSP70 plasmid into C4-2B cells and the HSP70 shRNA plasmid into ENZR-C4-2B cells, respectively. We observed a significant increase in AR-V7 expression upon overexpression of HSP70, whereas knockdown of HSP70 led to a significant decrease in AR-V7 expression, consistent with previous findings (Fig. S4A, B). Furthermore, in ENZR-C4-2B cells, simultaneous downregulation of 75aa and overexpression of HSP70 resulted in a significant increase in AR-V7 expression and inhibited degradation compared to 75aa knockdown alone, leading to enhanced resistance to ENZ (Fig. 7A–C; Fig. S4C, D). Conversely, in C4-2B cells, overexpression of 75aa and knockdown of HSP70 led to a significant decrease in AR-V7 expression and promoted degradation compared to 75aa overexpression alone, resulting in reduced resistance to ENZ (Fig. 7D–F; Fig. S4E, F). Additionally, in ENZR-C4-2B cells, we observed that 75aa inhibited the ability of STUB1 to degrade AR-V7 (Fig. 7G). These findings suggest that 75aa enhances the stability of HSP70 protein within the HSP70-STUB1 complex, thereby increasing AR-V7 expression and enhancing CRPC resistance to ENZ (Fig. 7H).

eIF4A3 and DDX39A collaboratively facilitate the expression of circSRCAP in CRPC cells.

The formation of circRNAs involves multiple splicing factors that regulate the generation of circRNAs through the reverse splicing of pre-mRNA. eIF4A3, a potent splicing factor, participates in various cancer progressions by positively or negatively regulating circRNA generation [45, 49–52]. In comparison to C4-2B cells, eIF4A3 expression significantly decreases in ENZR-C4-2B cells (Fig. S5A). Utilizing CircInteractome, we predicted eIF4A3 binding sites matching the circSRCAP flanking region, revealing four upstream and two downstream binding sites of eIF4A3 relative to circSRCAP mRNA (Fig. 8A). RIP assays using an anti-eIF4A3 antibody demonstrated eIF4A3's ability to bind to circSRCAP mRNA via three upstream putative binding sites (b, c, and d) within the corresponding RNA–protein complex, while no binding was observed in the downstream region (Fig. 8A). RNA truncation upstream of circSRCAP, followed by verification through RNA pull-down experiments, confirmed the necessity of these binding sites for the interaction between the circSRCAP upstream sequence and eIF4A3 (Fig. 8B). Furthermore, knockdown of eIF4A3 in ENZR-C4-2B cells significantly upregulated circSRCAP expression (Fig. 8C, D).

The site where circRNAs encode proteins or peptides is primarily the cytoplasm, prompting researchers to identify the (RBPs) that mediate their export from the nucleus. Through MS2-RIP combined with LC–MS, we identified that DDX39A protein can bind to circSRCAP (Fig. 8E). Notably, the expression of DDX39A in ENZR-C4-2B cells was significantly higher compared to C4-2B cells (Fig. S5B). Previous studies have suggested that DDX39A mediates the export of circRNAs from the nucleus [53]. In our study, overexpression of DDX39A notably increased the cytoplasmic content of circSRCAP while decreasing its nuclear content, whereas knockdown of DDX39A had the opposite effect (Fig. 8F). Immunofluorescence combined with FISH experiments demonstrated the colocalization of DDX39A and circSRCAP in the nucleus, with high or low expression of DDX39A affecting the distribution of circSRCAP within the cell (Fig. 8G). Collectively, these findings confirm that low expression of eIF4A3 in CRPC cells can enhance circSRCAP production, while DDX39A promotes the export of circSRCAP from the nucleus (Fig. 8H).

(See figure on next page.)

Fig. 6 75aa inhibits HSP70 protein degradation and formation of the HSP70-STUB1 complex. **A**,**B** Western blot analysis of HSP70 protein expression in C4-2B cells transfected with vector, circSRCAP overexpression plasmids, scramble or circSRCAP shRNAs. **C** Western blot detection of HSP70 in C4-2B cells transfected with vector, Flag-circSRCAP, Flag-Mut, or Flag-75aa plasmids. **D** Half-life of HSP70 in ENZR-C4-2B cells transfected with scramble or circSRCAP shRNAs, followed by 50 μg/mL cycloheximide (CHX) treatment and Western blot analysis at 0, 2, 4, and 8 h. **E** Immunoprecipitation of HSP70 from ENZR-C4-2B cells transfected with HA-Ub and scramble or circSRCAP shRNAs, followed by 5 μM MG132 treatment and Western blot detection. **F** Immunoprecipitation of HSP70 or STUB1 from total lysates of ENZR-C4-2B cells transfected with scramble or circSRCAP shRNAs, followed by Western blot. **G** Half-life of HSP70 in C4-2B cells transfected with vector or Flag-circSRCAP plasmids, followed by 50 μg/mL CHX treatment and Western blot analysis at 0, 2, 4, and 8 h. **H** Immunoprecipitation of HSP70 from C4-2B cells transfected with HA-Ub and vector or Flag-circSRCAP plasmids, followed by 5 μM MG132 treatment and Western blot. **I** Immunoprecipitation of HSP70 or STUB1 from total lysates of C4-2B cells transfected with vector or Flag-circSRCAP plasmids, followed by Western blot

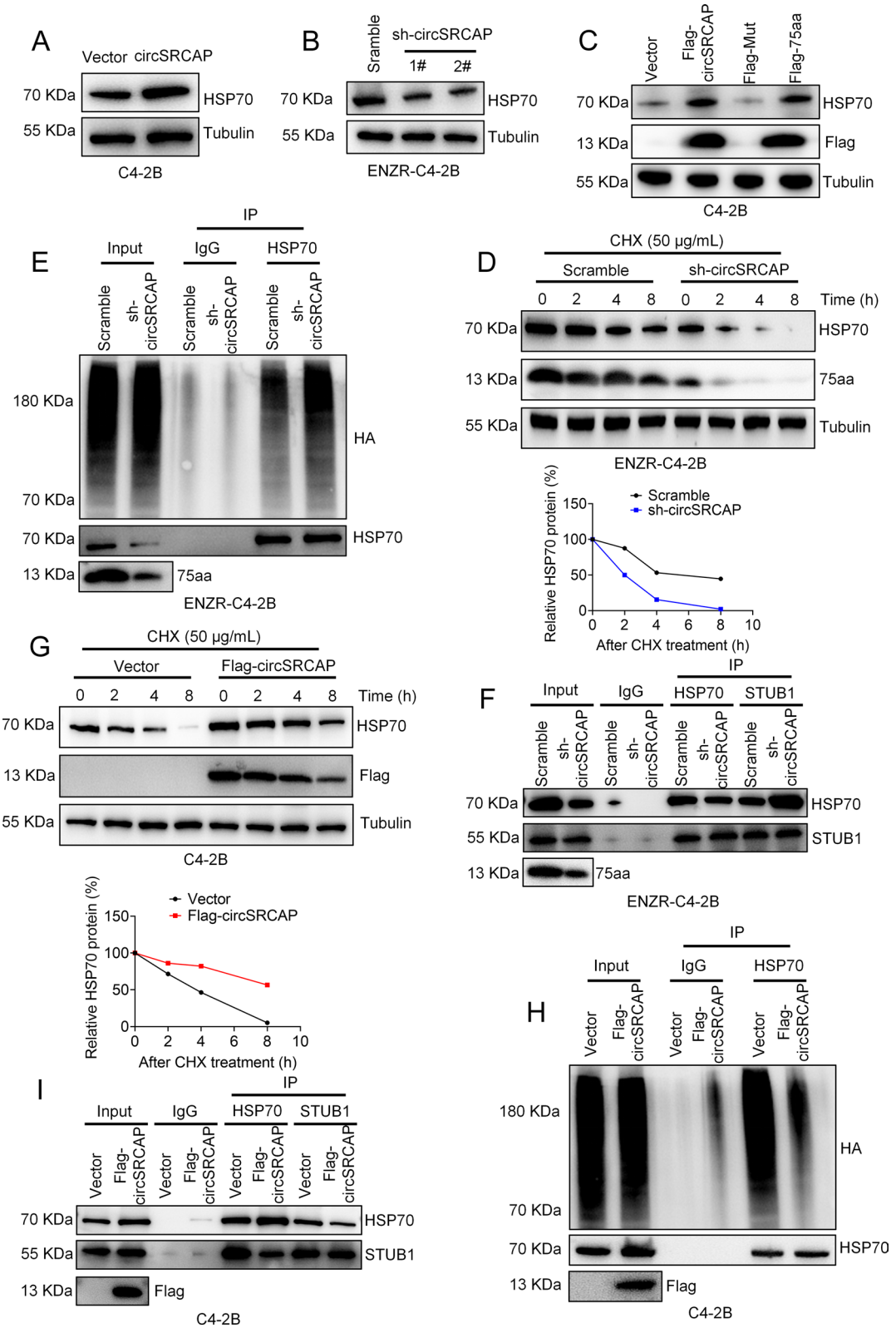

Fig. 6 (See legend on previous page.)

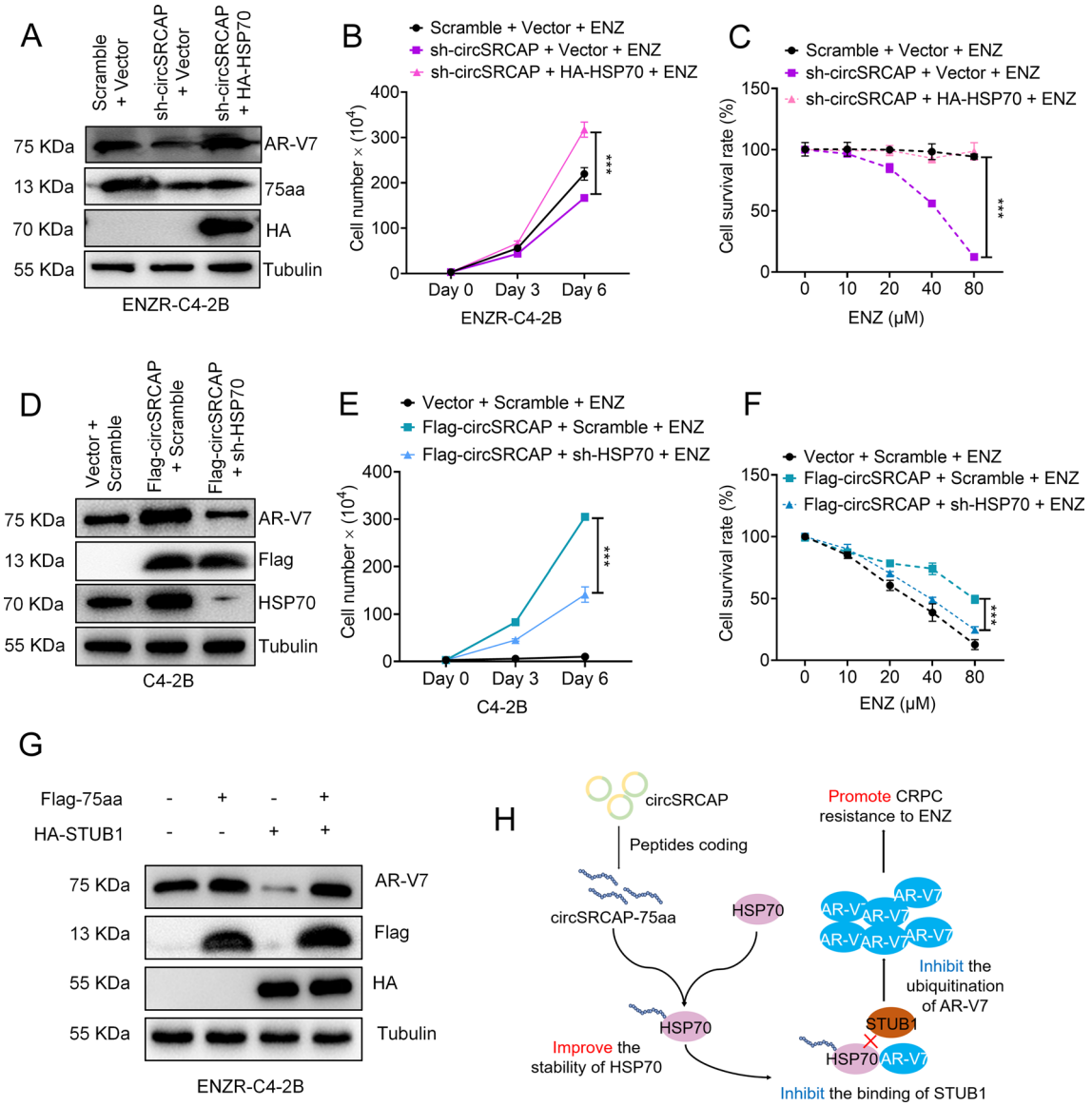

Fig. 7 75aa regulates AR-V7 expression via the HSP70-STUB1 complex. **A** AR-V7 expression in ENZR-C4-2B cells transfected with scramble + vector, sh-circSRCAP + vector, or sh-circSRCAP + HA-HSP70 plasmids, detected by Western blot. **B** Total cell count in ENZR-C4-2B cells transfected with scramble + vector, sh-circSRCAP + vector, or sh-circSRCAP + HA-HSP70 plasmids, after treatment with 10 μM ENZ for 0, 3, and 6 days. **C** Total cell count in ENZR-C4-2B cells transfected with scramble + vector, sh-circSRCAP + vector, or sh-circSRCAP + HA-HSP70 plasmids, treated with different ENZ concentrations for 3 days. **D** AR-V7 expression in C4-2B cells transfected with vector + scramble, Flag-circSRCAP + scramble, or Flag-circSRCAP + sh-HSP70 plasmids, detected by Western blot. **E** Total cell count in C4-2B cells transfected with vector + scramble, Flag-circSRCAP + scramble, or Flag-circSRCAP + sh-HSP70 plasmids, after treatment with 10 μM ENZ for 0, 3, and 6 days. **F** Total cell count in C4-2B cells transfected with vector + scramble, Flag-circSRCAP + scramble, or Flag-circSRCAP + sh-HSP70 plasmids, treated with different ENZ concentrations for 3 days. **G** AR-V7 expression in ENZR-C4-2B cells transfected with Flag-75aa, HA-STUB1, or Flag-75aa + HA-STUB1 plasmids, detected by Western blot. **H** Schematic illustrating the role of circSRCAP in CRPC resistance to ENZ. Statistical significance was determined by one-way ANOVA (*** $p < 0.001$)

Discussion

CRPC, a fatal male disease, primarily relies on AR inhibitors for clinical treatment, yet available options remain limited [54–57]. Drug resistance often emerges due to abnormal AR splicing following endocrine therapy, posing a significant challenge in CRPC management [58–60]. To address this, novel treatment strategies and biomarkers are urgently needed. Here, we identify circSRCAP, a previously unexplored circRNA derived from exons 26–27 of the SRCAP gene, as upregulated in

ENZR-C4-2B cells, correlating with heightened AR-V7 expression and ENZ resistance. Our findings reveal that circSRCAP encodes a 75aa peptide via an active IRES. In vitro assays demonstrate that 75aa, not circSRCAP itself, promotes CRPC resistance to ENZ. Mechanistically, 75aa inhibits STUB1-mediated ubiquitination of AR-V7 protein by directly binding to HSP70, sustaining AR-V7 expression in ENZR-CRPC. Furthermore, we elucidate that the splicing factor eIF4A3 regulates circSRCAP generation by binding to its precursor mRNA, while RBP DDX39A mediates circSRCAP export from the nucleus, facilitating 75aa encoding. Overall, our findings propose circSRCAP as a potential therapeutic target for ENZR-CRPC.

While our research demonstrates that knockdown of circSRCAP and 75aa reduces ENZR-CRPC resistance to ENZ in xenograft models and weakens ENZ tolerance in ENZR-C4-2B cells in vitro, our study lacks human pathological tissue samples to verify 75aa expression in ENZR-CRPC patients. This leaves the expression of circSRCAP and 75aa in ENZR-CRPC patients uncertain, and it's unclear if 75aa's role in humans solely involves regulating the HSP70-STUB1 complex. Notably, AR-Vs cleavage is a crucial aspect of CRPC resistance to endocrine therapy, but it's not the sole determinant. Prior to ENZ treatment, 75% of CRPC patients on ADT alone express nuclear AR-V7, yet ENZA treatment yields significant antitumor activity, with response rates ranging from 57 to 78% [13, 14, 60, 61]. These data suggest that AR-V7 protein expression in tissues does not conclusively indicate CRPC's absolute treatment intolerance. Hence, further exploration is needed to uncover additional mechanisms through which 75aa promotes CRPC resistance to ENZ, and our ongoing research endeavors are addressing this aspect. However, in addition to ENZ, second-generation androgen receptor inhibitors, including apalutamide and revilutamide, also target the androgen receptor (AR) and its signaling pathways.

In various disease models, circRNAs have predominantly been studied for their role as "microRNA sponges" [62–65]. However, only a handful of studies have investigated the involvement of circRNAs in regulating CRPC cell resistance to ENZ, and none of them have explored the translational function of circRNAs [66–68]. With advancements in bioinformatics, researchers can now predict circRNAs potentially capable of encoding proteins or peptides driven by specific IRES or N6-methyladenosine (m6A) modifications, some of which have been recently reported [69–71]. This prompted us to investigate the possibility and molecular effects of circSRCAP-derived translated proteins or peptides on CRPC resistance to ENZ. Upon evaluating circSRCAP's sequence on the circRNADb website, we predicted and obtained its putative IRES structure and ORF, indicating its potential to encode small peptides [72]. As IRES serves as a crucial promoter for circRNA translation, we constructed a circSRCAP IRES truncation plasmid to compare its expression with the predicted wild-type circSRCAP IRES plasmid. Our findings demonstrated that circSRCAP possesses the translation initiation ability and polypeptide coding potential of IRES. Through a series of experiments, we further validated that the 75aa polypeptide encoded by circSRCAP, rather than circSRCAP itself, promotes CRPC cell resistance to ENZ.

STUB1, an essential E3 ubiquitin ligase, regulates multiple nuclear receptors [73–75]. Its interaction with AR/AR-V7 enhances their ubiquitination and degradation, underscoring its significance in controlling oncogenic proteins. HSP70, a co-chaperone protein of AR-V7, facilitates its maturation by forming a complex with AR-V7. However, STUB1 disrupts this complex formation, leading to AR/AR-V7 protein degradation. Targeting HSP70 strengthens the binding between STUB1 and AR/AR-V7, promoting their ubiquitination and degradation. The HSP70-STUB1 complex represents a fundamental chaperone-ubiquitin–proteasome mechanism governing AR variant protein stability, offering a potential strategy to combat CRPC drug resistance [36]. HSP70, comprising an N-terminal ATPase domain and a C-terminal substrate binding domain, along with HSP40, aids in the degradation of misfolded proteins [76–78]. STUB1 mediates HSP70

(See figure on next page.)

Fig. 8 eIF4A3 and DDX39A collaboratively facilitate the expression of circSRCAP in CRPC cells. **A** Predicted binding sites of eIF4A3 in the flanking regions of circSRCAP (upper) and RIP validation of the binding site on the circSRCAP upstream sequence (lower). **B** RNA pull-down experiments to analyze the interaction between eIF4A3 and circSRCAP upstream truncates. Laz was used as a negative control and H19 as a positive control. **C** Western blot analysis of eIF4A3 expression in ENZR-C4-2B cells transfected with scramble or eIF4A3 shRNAs. **D** qRT-PCR analysis of circSRCAP expression in ENZR-C4-2B cells transfected with scramble or eIF4A3 shRNAs. **E** MS2-RIP assay schematic (upper left), with DDX39A protein identified by LC–MS (right and lower left panels). **F** qRT-PCR to investigate the distribution of circSRCAP in the nucleus and cytoplasm of ENZR-C4-2B cells transfected with vector, DDX39A overexpression, scramble, or DDX39A shRNAs, with U6 and GAPDH as nuclear and cytoplasmic markers, respectively. **G** Immunofluorescence and FISH analysis of DDX39A and circSRCAP colocalization in ENZR-C4-2B cells transfected with vector, DDX39A overexpression, scramble, or DDX39A shRNAs. Scale bar = 10 μm. **H** Schematic representation of the cooperative role of eIF4A3 and DDX39A in promoting circSRCAP expression. Statistical significance was determined by one-way ANOVA (** $p < 0.01$, *** $p < 0.001$)

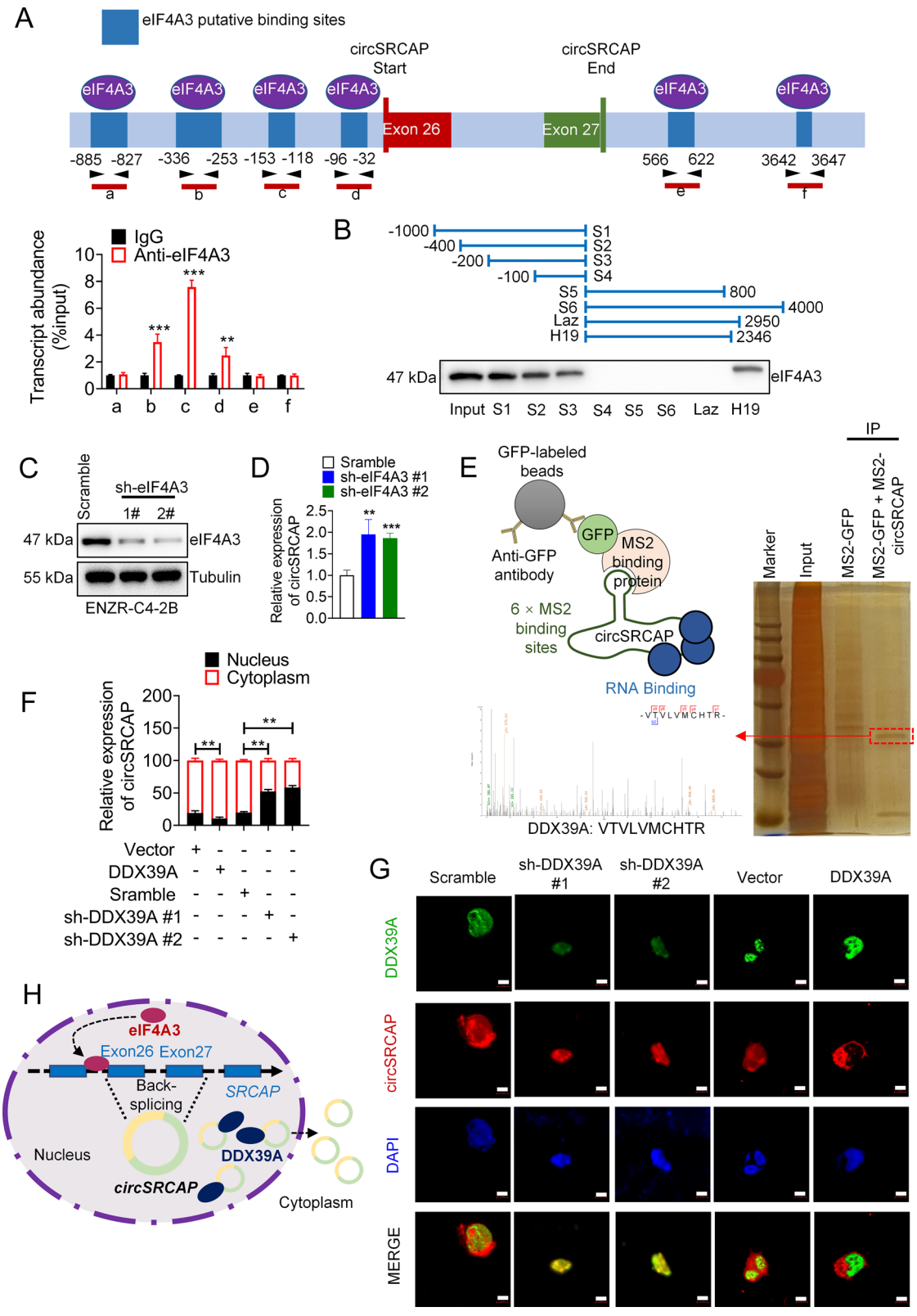

Fig. 8 (See legend on previous page.)

degradation post-misfolded protein degradation, maintaining its optimal levels [79]. Abnormal HSP70 overexpression is observed in CRPC and mCRPC, correlating with high Gleason scores in PC and AR-V7 levels [36, 80–82]. The HSP70/STUB1 complex homeostasis may crucially modulate AR-V7 protein levels, where HSP70 binds to AR-V7, shielding it from STUB1-mediated degradation. This study affirms 75aa as the driving force behind elevated HSP70 protein expression. At a deeper level, AR-V7 can also mediate the resistance to CRPC induced by second-generation androgen receptor inhibitors, such as apalutamide and darolutamide, in the same manner as ENZ. Moreover, beyond the second-generation androgen receptor inhibitors, the HSP70/STUB1 complex can regulate the activity of CRPC cells resistant to abiraterone. These findings suggest that the 75aa peptide may not only target ENZ-induced CRPC but also potentially offer therapeutic benefits in CRPC resistance driven by other endocrine therapies. Hence, targeting the 75aa peptide derived from circSRCAP holds promise as a potential therapeutic avenue for AR-V7-overexpressing CRPC patients.

The biogenesis of circRNAs involves intricate processes, with the involvement of various RBPs adding to its complexity. Several RBPs have been reported to either promote or inhibit circRNA biogenesis. For instance, QKI enhances circRNA production by binding to specific single-stranded RNA motifs in flanking introns during EMT, while ADAR1 inhibits circRNA expression through A-to-I editing of RNA pairs neighboring the circular exon [83, 84]. However, the functions and mechanisms of many other RBPs in circRNA biogenesis remain elusive. In this study, we discovered that eIF4A3 negatively regulates circSRCAP expression in ENZR-CRPC cells. Notably, our findings suggest a negative correlation between eIF4A3 and circSRCAP expression. Despite reports indicating that eIF4A3 can both promote and inhibit circRNA expression, its specific regulatory mechanisms remain unclear [51, 85]. The export of circRNA from the nucleus is crucial for its coding function. Here, we identified DDX39A as a key RBP mediating circSRCAP nuclear export using MS2-RIP combined with LC–MS. DDX39A has been recognized as a pivotal regulator of RNA export from the nucleus and is primarily involved in exporting circRNAs shorter than 400 nt [86, 87]. Indeed, prior studies have primarily relied on DDX39A knockdown to assess the distribution of circRNAs of varying lengths across different cellular compartments. However, this approach may not fully capture the comprehensive impact of DDX39A on all circRNAs within different length ranges. Additionally, the specific regulatory mechanisms through which DDX39A mediates circRNA nuclear export have yet to be fully elucidated. Therefore, further research is needed to explore the broader role of DDX39A in circRNA biology and to uncover the precise mechanisms underlying its involvement in circRNA nuclear export. Our research underscores DDX39A as a critical RBP mediating circSRCAP nuclear export, thereby endowing it with coding potential. Overall, our findings shed new light on the role of DDX39A in controlling circRNA nuclear export, offering a fresh perspective on its regulatory mechanisms in circRNA biology.

We have conclusively demonstrated for the first time that the 75aa peptide is encoded by circSRCAP, exhibiting upregulation in ENZR-CRPC cells and possessing coding capability. Notably, reducing the expression of the 75aa peptide, without altering circSRCAP expression, sensitized ENZR-C4-2B cells to ENZ in vitro. Mechanistically, 75aa directly interacts with the DR structure of HSP70, disrupting the formation of the HSP70-STUB1 complex and thereby impeding AR-V7 degradation via the ubiquitin–proteasome pathway, consequently promoting CRPC resistance to ENZ. Moreover, the downregulation of eIF4A3 facilitates unimpeded production of circSRCAP in ENZR-CRPC cells, augmenting its expression, while DDX39A facilitates the nuclear export of circSRCAP, thereby facilitating the encoding of the 75aa peptide. In summary, targeting the 75aa peptide presents a promising therapeutic avenue to enhance the sensitivity of ENZR-CRPC patients to ENZ.

Conclusions

In conclusion, circSRCAP plays a crucial role in bolstering the resistance of CRPC cells to ENZR through the encoding of a novel 75aa peptide, which acts on the HSP70-STUB1 complex to augment the stability of AR-V7. In addition, the generation of circSRCAP is regulated by eIF4A3 and mediated by DDX39A for export from the nucleus. Overall, the revelation of circSRCAP's coding function expands our comprehension of circRNA involvement in the development and resistance mechanisms of ENZR-CRPC.

Abbreviations

AR-V7	Androgen receptor splice variant-7
CRPC	Castration-resistant prostate cancer
AR	Androgen
ENZ	Enzalutamide
circRNA	Circular RNA
ENZR-C4-2B	ENZ-resistant C4-2B
ENZR-CRPC	ENZ-resistant CRPC
ADT	Androgen deprivation therapy
ABI	Abiraterone acetate
LBD	Ligand binding domain
HSP	Heat shock protein
STUB1	STIP1 homology and U-box containing protein 1
75aa	CircSRCAP-75aa
eIF4A3	Eukaryotic translation initiation factor 4A3
DDX39A	DExD-box helicase 39A

Co-IP	Co-immunoprecipitation
CHX	Cycloheximide
FISH	Fluorescence in situ hybridization
LC-MS	Liquid chromatography-tandem mass spectrometry
RIP	RNA Immunoprecipitation
IHC	Immunohistochemical

Supplementary Information

The online version contains supplementary material available at https://doi.org/10.1186/s12967-025-06115-z.

Additional file 1.

Additional file 2.

Additional file 3.

Additional file 4.

Additional file 5.

Additional file 6.

Additional file 7.

Author contributions

JB, HG and SQ conceived of the study. XM and QW performed the experiments. XM and CC conducted the statistical analyses. WY and SC helped a portion of experiment design. XM and QW wrote the paper and JB revised the paper. All authors approved the manuscript.

Funding

This work was supported by National Natural Science Foundation of China (82202856), China Postdoctoral Science Foundation (2021M702754) and Key project of Xuzhou Municipal Health Commission (XWKYHT20210589).

Availability of data and material

All the data supporting the findings of this study are available within the article and its supplementary information files and from the corresponding author upon reasonable request.

Declarations

Ethics approval and consent to participate

The animal experimental procedures involving mice were carried out as prescribed by the National Guidelines for Animal Usage in Research (China) and were approved by the Institutional Animal Care and Use Committee of Xuzhou Medical University (202309T023). This study was conducted following approval by the Institutional Animal Care and Use Committee of Xuzhou Medical University (202309T023). All treatments were administered in accordance with the guidelines established by the committee.

Consent for publication

All authors consent to publication.

Competing interests

The authors have declared that no competing interest exists.

Author details

[1]Cancer Institute, Xuzhou Medical University, 209 Tongshan Road, Xuzhou 221004, Jiangsu, China. [2]Center of Clinical Oncology, The Affiliated Hospital of Xuzhou Medical University, Xuzhou, Jiangsu, China. [3]Jiangsu Center for the Collaboration and Innovation of Cancer Biotherapy, Cancer Institute, Xuzhou Medical University, Xuzhou, Jiangsu, China. [4]School of Medical Technology, Xuzhou Key Laboratory of Laboratory Diagnostics, Xuzhou Medical University, 209 Tongshan Road, Xuzhou 221004, Jiangsu, China. [5]Department of Oncology, Xuzhou Central Hospital, Xuzhou, Jiangsu, China. [6]Department of Oncology, Xuzhou Institute of Medical Science, Xuzhou, Jiangsu, China. [7]Department of General Surgery, Xi'an Central Hospital, Xi'an 710004, Shaanxi, China.

Received: 19 September 2024 Accepted: 8 January 2025
Published online: 23 January 2025

References

1. Siegel RL, Miller KD, Wagle NS, Jemal A. Cancer statistics, 2023. CA Cancer J Clin. 2023;73:17–48.
2. Visakorpi T, Hyytinen E, Koivisto P, Tanner M, Keinanen R, Palmberg C, et al. In vivo amplification of the androgen receptor gene and progression of human prostate cancer. Nat Genet. 1995;9:401–6.
3. Robinson D, Van Allen EM, Wu YM, Schultz N, Lonigro RJ, Mosquera JM, et al. Integrative clinical genomics of advanced prostate cancer. Cell. 2015;162:454.
4. Chen CD, Welsbie DS, Tran C, Baek SH, Chen R, Vessella R, et al. Molecular determinants of resistance to antiandrogen therapy. Nat Med. 2004;10:33–9.
5. Kumar A, Coleman I, Morrissey C, Zhang X, True LD, Gulati R, et al. Substantial interindividual and limited intraindividual genomic diversity among tumors from men with metastatic prostate cancer. Nat Med. 2016;22:369–78.
6. Ritch CR, Cookson MS. Advances in the management of castration resistant prostate cancer. BMJ. 2016;355: i4405.
7. Romanel A, Gasi Tandefelt D, Conteduca V, Jayaram A, Casiraghi N, Wetterskog D, et al. Plasma AR and abiraterone-resistant prostate cancer. Sci Transl Med. 2015;7:312re10.
8. Conteduca V, Wetterskog D, Sharabiani MTA, Grande E, Fernandez-Perez MP, Jayaram A, et al. Androgen receptor gene status in plasma DNA associates with worse outcome on enzalutamide or abiraterone for castration-resistant prostate cancer: a multi-institution correlative biomarker study. Ann Oncol. 2017;28:1508–16.
9. Cato L, Neeb A, Sharp A, Buzon V, Ficarro SB, Yang L, et al. Development of Bag-1L as a therapeutic target in androgen receptor-dependent prostate cancer. Elife. 2017;6: e27159.
10. Linja MJ, Savinainen KJ, Saramaki OR, Tammela TL, Vessella RL, Visakorpi T. Amplification and overexpression of androgen receptor gene in hormone-refractory prostate cancer. Cancer Res. 2001;61:3550–5.
11. Fizazi K, Scher HI, Miller K, Basch E, Sternberg CN, Cella D, et al. Effect of enzalutamide on time to first skeletal-related event, pain, and quality of life in men with castration-resistant prostate cancer: results from the randomised, phase 3 AFFIRM trial. Lancet Oncol. 2014;15:1147–56.
12. James ND, de Bono JS, Spears MR, Clarke NW, Mason MD, Dearnaley DP, et al. Abiraterone for prostate cancer not previously treated with hormone therapy. N Engl J Med. 2017;377:338–51.
13. Beer TM, Tombal B. Enzalutamide in metastatic prostate cancer before chemotherapy. N Engl J Med. 2014;371:1755–6.
14. Ryan CJ, Smith MR, de Bono JS, Molina A, Logothetis CJ, de Souza P, et al. Abiraterone in metastatic prostate cancer without previous chemotherapy. N Engl J Med. 2013;368:138–48.
15. Loriot Y, Miller K, Sternberg CN, Fizazi K, De Bono JS, Chowdhury S, et al. Effect of enzalutamide on health-related quality of life, pain, and skeletal-related events in asymptomatic and minimally symptomatic, chemotherapy-naive patients with metastatic castration-resistant prostate cancer (PREVAIL): results from a randomised, phase 3 trial. Lancet Oncol. 2015;16:509–21.
16. Fizazi K, Tran N, Fein L, Matsubara N, Rodriguez-Antolin A, Alekseev BY, et al. Abiraterone plus prednisone in metastatic, castration-sensitive prostate cancer. N Engl J Med. 2017;377:352–60.
17. De Laere B, van Dam PJ, Whitington T, Mayrhofer M, Diaz EH, Van den Eynden G, et al. Comprehensive profiling of the androgen receptor in liquid biopsies from castration-resistant prostate cancer reveals novel intra-AR structural variation and splice variant expression patterns. Eur Urol. 2017;72:192–200.
18. Guo Z, Yang X, Sun F, Jiang R, Linn DE, Chen H, et al. A novel androgen receptor splice variant is up-regulated during prostate cancer progression and promotes androgen depletion-resistant growth. Cancer Res. 2009;69:2305–13.
19. Hu R, Lu C, Mostaghel EA, Yegnasubramanian S, Gurel M, Tannahill C, et al. Distinct transcriptional programs mediated by the ligand-dependent full-length androgen receptor and its splice variants in castration-resistant prostate cancer. Cancer Res. 2012;72:3457–62.

20. Li Y, Chan SC, Brand LJ, Hwang TH, Silverstein KA, Dehm SM. Androgen receptor splice variants mediate enzalutamide resistance in castration-resistant prostate cancer cell lines. Cancer Res. 2013;73:483–9.
21. Antonarakis ES, Lu C, Wang H, Luber B, Nakazawa M, Roeser JC, et al. AR-V7 and resistance to enzalutamide and abiraterone in prostate cancer. N Engl J Med. 2014;371:1028–38.
22. Guedes LB, Morais CL, Almutairi F, Haffner MC, Zheng Q, Isaacs JT, et al. Analytic Validation of RNA In Situ Hybridization (RISH) for AR and AR-V7 Expression in human prostate cancer. Clin Cancer Res. 2016;22:4651–63.
23. Nakazawa M, Lu C, Chen Y, Paller CJ, Carducci MA, Eisenberger MA, et al. Serial blood-based analysis of AR-V7 in men with advanced prostate cancer. Ann Oncol. 2015;26:1859–65.
24. Qu F, Xie W, Nakabayashi M, Zhang H, Jeong SH, Wang X, et al. Association of AR-V7 and prostate-specific antigen RNA levels in blood with efficacy of abiraterone acetate and enzalutamide treatment in men with prostate cancer. Clin Cancer Res. 2017;23:726–34.
25. Scher HI, Graf RP, Schreiber NA, McLaughlin B, Lu D, Louw J, et al. Nuclear-specific AR-V7 protein localization is necessary to guide treatment selection in metastatic castration-resistant prostate cancer. Eur Urol. 2017;71:874–82.
26. Scher HI, Lu D, Schreiber NA, Louw J, Graf RP, Vargas HA, et al. Association of AR-V7 on circulating tumor cells as a treatment-specific biomarker with outcomes and survival in castration-resistant prostate cancer. JAMA Oncol. 2016;2:1441–9.
27. Welti J, Rodrigues DN, Sharp A, Sun S, Lorente D, Riisnaes R, et al. Analytical validation and clinical qualification of a new immunohistochemical assay for androgen receptor splice variant-7 protein expression in metastatic castration-resistant prostate cancer. Eur Urol. 2016;70:599–608.
28. Zhu Y, Sharp A, Anderson CM, Silberstein JL, Taylor M, Lu C, et al. Novel junction-specific and quantifiable in situ detection of AR-V7 and its clinical correlates in metastatic castration-resistant prostate cancer. Eur Urol. 2018;73:727–35.
29. Liu LL, Xie N, Sun S, Plymate S, Mostaghel E, Dong X. Mechanisms of the androgen receptor splicing in prostate cancer cells. Oncogene. 2014;33:3140–50.
30. Nyquist MD, Li Y, Hwang TH, Manlove LS, Vessella RL, Silverstein KA, et al. TALEN-engineered AR gene rearrangements reveal endocrine uncoupling of androgen receptor in prostate cancer. Proc Natl Acad Sci USA. 2013;110:17492–7.
31. Hu R, Dunn TA, Wei S, Isharwal S, Veltri RW, Humphreys E, et al. Ligand-independent androgen receptor variants derived from splicing of cryptic exons signify hormone-refractory prostate cancer. Cancer Res. 2009;69:16–22.
32. Whitesell L, Lindquist SL. HSP90 and the chaperoning of cancer. Nat Rev Cancer. 2005;5:761–72.
33. Hartl FU, Bracher A, Hayer-Hartl M. Molecular chaperones in protein folding and proteostasis. Nature. 2011;475:324–32.
34. Powers MV, Clarke PA, Workman P. Dual targeting of HSC70 and HSP72 inhibits HSP90 function and induces tumor-specific apoptosis. Cancer Cell. 2008;14:250–62.
35. Meimaridou E, Gooljar SB, Chapple JP. From hatching to dispatching: the multiple cellular roles of the Hsp70 molecular chaperone machinery. J Mol Endocrinol. 2009;42:1–9.
36. Liu C, Lou W, Yang JC, Liu L, Armstrong CM, Lombard AP, et al. Proteostasis by STUB1/HSP70 complex controls sensitivity to androgen receptor targeted therapy in advanced prostate cancer. Nat Commun. 2018;9:4700.
37. Xiong L, Liu HS, Zhou C, Yang X, Huang L, Jie HQ, et al. A novel protein encoded by circINSIG1 reprograms cholesterol metabolism by promoting the ubiquitin-dependent degradation of INSIG1 in colorectal cancer. Mol Cancer. 2023;22:72.
38. Wang Z, Sun A, Yan A, Yao J, Huang H, Gao Z, et al. Circular RNA MTCL1 promotes advanced laryngeal squamous cell carcinoma progression by inhibiting C1QBP ubiquitin degradation and mediating beta-catenin activation. Mol Cancer. 2022;21:92.
39. Zheng L, Liang H, Zhang Q, Shen Z, Sun Y, Zhao X, et al. circPTEN1, a circular RNA generated from PTEN, suppresses cancer progression through inhibition of TGF-beta/Smad signaling. Mol Cancer. 2022;21:41.
40. Shi X, Yang J, Liu M, Zhang Y, Zhou Z, Luo W, et al. Circular RNA ANAPC7 inhibits tumor growth and muscle wasting via PHLPP2-AKT-TGF-beta signaling axis in pancreatic cancer. Gastroenterology. 2022;162(2004–17):e2.
41. Chen R, Yang T, Jin B, Xu W, Yan Y, Wood N, et al. CircTmeff1 promotes muscle atrophy by interacting with TDP-43 and encoding a novel TMEFF1-339aa protein. Adv Sci. 2023;10: e2206732.
42. Yu YZ, Lv DJ, Wang C, Song XL, Xie T, Wang T, et al. Hsa_circ_0003258 promotes prostate cancer metastasis by complexing with IGF2BP3 and sponging miR-653-5p. Mol Cancer. 2022;21:12.
43. Xie T, Fu DJ, Li ZM, Lv DJ, Song XL, Yu YZ, et al. CircSMARCC1 facilitates tumor progression by disrupting the crosstalk between prostate cancer cells and tumor-associated macrophages via miR-1322/CCL20/CCR6 signaling. Mol Cancer. 2022;21:173.
44. Ding L, Wang R, Zheng Q, Shen D, Wang H, Lu Z, et al. circPDE5A regulates prostate cancer metastasis via controlling WTAP-dependent N^6-methyladenisine methylation of EIF3C mRNA. J Exp Clin Cancer Res. 2022;41:187.
45. Jiang X, Guo S, Wang S, Zhang Y, Chen H, Wang Y, et al. EIF4A3-induced circARHGAP29 promotes aerobic glycolysis in docetaxel-resistant prostate cancer through IGF2BP2/c-Myc/LDHA signaling. Cancer Res. 2022;82:831–45.
46. Liu C, Lou W, Zhu Y, Nadiminty N, Schwartz CT, Evans CP, et al. Niclosamide inhibits androgen receptor variants expression and overcomes enzalutamide resistance in castration-resistant prostate cancer. Clin Cancer Res. 2014;20:3198–210.
47. Gao X, Xia X, Li F, Zhang M, Zhou H, Wu X, et al. Circular RNA-encoded oncogenic E-cadherin variant promotes glioblastoma tumorigenicity through activation of EGFR-STAT3 signalling. Nat Cell Biol. 2021;23:278–91.
48. Lei M, Zheng G, Ning Q, Zheng J, Dong D. Translation and functional roles of circular RNAs in human cancer. Mol Cancer. 2020;19:30.
49. Zheng X, Huang M, Xing L, Yang R, Wang X, Jiang R, et al. The circRNA circSEPT9 mediated by E2F1 and EIF4A3 facilitates the carcinogenesis and development of triple-negative breast cancer. Mol Cancer. 2020;19:73.
50. Hu Z, Chen G, Zhao Y, Gao H, Li L, Yin Y, et al. Exosome-derived circCCAR1 promotes $CD8^+$ T-cell dysfunction and anti-PD1 resistance in hepatocellular carcinoma. Mol Cancer. 2023;22:55.
51. Wei Y, Lu C, Zhou P, Zhao L, Lyu X, Yin J, et al. EIF4A3-induced circular RNA ASAP1 promotes tumorigenesis and temozolomide resistance of glioblastoma via NRAS/MEK1/ERK1-2 signaling. Neuro Oncol. 2021;23:611–24.
52. Yang M, Hu H, Wu S, Ding J, Yin B, Huang B, et al. EIF4A3-regulated circ_0087429 can reverse EMT and inhibit the progression of cervical cancer via miR-5003-3p-dependent upregulation of OGN expression. J Exp Clin Cancer Res. 2022;41:165.
53. Huang C, Liang D, Tatomer DC, Wilusz JE. A length-dependent evolutionarily conserved pathway controls nuclear export of circular RNAs. Genes Dev. 2018;32:639–44.
54. Francolini G, Allegra AG, Detti B, Di Cataldo V, Caini S, Bruni A, et al. Stereotactic body radiation therapy and abiraterone acetate for patients affected by oligometastatic castrate-resistant prostate cancer: a randomized phase II trial (ARTO). J Clin Oncol. 2023;41:5561–8.
55. Qin X, Ji D, Gu W, Han W, Luo H, Du C, et al. Activity and safety of SHR3680, a novel antiandrogen, in patients with metastatic castration-resistant prostate cancer: a phase I/II trial. BMC Med. 2022;20:84.
56. Szmulewitz RZ, Peer CJ, Ibraheem A, Martinez E, Kozloff MF, Carthon B, et al. Prospective international randomized phase II study of low-dose abiraterone with food versus standard dose abiraterone in castration-resistant prostate cancer. J Clin Oncol. 2018;36:1389–95.
57. Small EJ, Saad F, Chowdhury S, Oudard S, Hadaschik BA, Graff JN, et al. Apalutamide and overall survival in non-metastatic castration-resistant prostate cancer. Ann Oncol. 2019;30:1813–20.
58. He Y, Wei T, Ye Z, Orme JJ, Lin D, Sheng H, et al. A noncanonical AR addiction drives enzalutamide resistance in prostate cancer. Nat Commun. 2021;12:1521.
59. Cai M, Song XL, Li XA, Chen M, Guo J, Yang DH, et al. Current therapy and drug resistance in metastatic castration-resistant prostate cancer. Drug Resist Updates. 2023;68: 100962.
60. Sharp A, Coleman I, Yuan W, Sprenger C, Dolling D, Rodrigues DN, et al. Androgen receptor splice variant-7 expression emerges with castration resistance in prostate cancer. J Clin Invest. 2019;129:192–208.
61. Attard G, Reid AH, Yap TA, Raynaud F, Dowsett M, Settatree S, et al. Phase I clinical trial of a selective inhibitor of CYP17, abiraterone acetate, confirms that castration-resistant prostate cancer commonly remains hormone driven. J Clin Oncol. 2008;26:4563–71.

62. Zhang D, Ni N, Wang Y, Tang Z, Gao H, Ju Y, et al. CircRNA-vgll3 promotes osteogenic differentiation of adipose-derived mesenchymal stem cells via modulating miRNA-dependent integrin alpha5 expression. Cell Death Differ. 2021;28:283–302.
63. Zhao C, Qian S, Tai Y, Guo Y, Tang C, Huang Z, et al. Proangiogenic role of circRNA-007371 in liver fibrosis. Cell Prolif. 2023;56: e13432.
64. Wang G, Cheng T, Yuan H, Zou F, Miao P, Jiao J. Tracing cellular interaction of circRNA-miRNA axis with Cu metal-organic framework supported DNA cascade assembly. Biosens Bioelectron. 2023;228: 115226.
65. Long F, Li L, Xie C, Ma M, Wu Z, Lu Z, et al. Intergenic CircRNA Circ_0007379 inhibits colorectal cancer progression by modulating miR-320a biogenesis in a KSRP-dependent manner. Int J Biol Sci. 2023;19:3781–803.
66. Greene J, Baird AM, Casey O, Brady L, Blackshields G, Lim M, et al. Circular RNAs are differentially expressed in prostate cancer and are potentially associated with resistance to enzalutamide. Sci Rep. 2019;9:10739.
67. Chen L, Sun Y, Tang M, Wu D, Xiang Z, Huang CP, et al. High-dose-androgen-induced autophagic cell death to suppress the enzalutamide-resistant prostate cancer growth via altering the circRNA-BCL2/miRNA-198/AMBRA1 signaling. Cell Death Discov. 2022;8:128.
68. Wu G, Sun Y, Xiang Z, Wang K, Liu B, Xiao G, et al. Preclinical study using circular RNA 17 and micro RNA 181c–5p to suppress the enzalutamide-resistant prostate cancer progression. Cell Death Dis. 2019;10:37.
69. Li Y, Wang Z, Su P, Liang Y, Li Z, Zhang H, et al. circ-EIF6 encodes EIF6-224aa to promote TNBC progression via stabilizing MYH9 and activating the Wnt/beta-catenin pathway. Mol Ther. 2022;30:415–30.
70. Li P, Song R, Yin F, Liu M, Liu H, Ma S, et al. circMRPS35 promotes malignant progression and cisplatin resistance in hepatocellular carcinoma. Mol Ther. 2022;30:431–47.
71. Li Y, Chen B, Zhao J, Li Q, Chen S, Guo T, et al. HNRNPL circularizes ARHGAP35 to produce an oncogenic protein. Adv Sci. 2021;8:2001701.
72. Chen X, Han P, Zhou T, Guo X, Song X, Li Y. circRNADb: a comprehensive database for human circular RNAs with protein-coding annotations. Sci Rep. 2016;6:34985.
73. Rees I, Lee S, Kim H, Tsai FT. The E3 ubiquitin ligase CHIP binds the androgen receptor in a phosphorylation-dependent manner. Biochim Biophys Acta. 2006;1764:1073–9.
74. Chymkowitch P, Le May N, Charneau P, Compe E, Egly JM. The phosphorylation of the androgen receptor by TFIIH directs the ubiquitin/proteasome process. EMBO J. 2011;30:468–79.
75. Sarkar S, Brautigan DL, Parsons SJ, Larner JM. Androgen receptor degradation by the E3 ligase CHIP modulates mitotic arrest in prostate cancer cells. Oncogene. 2014;33:26–33.
76. Taipale M, Tucker G, Peng J, Krykbaeva I, Lin ZY, Larsen B, et al. A quantitative chaperone interaction network reveals the architecture of cellular protein homeostasis pathways. Cell. 2014;158:434–48.
77. Shiber A, Breuer W, Brandeis M, Ravid T. Ubiquitin conjugation triggers misfolded protein sequestration into quality control foci when Hsp70 chaperone levels are limiting. Mol Biol Cell. 2013;24:2076–87.
78. Peters LZ, Karmon O, David-Kadoch G, Hazan R, Yu T, Glickman MH, et al. The protein quality control machinery regulates its misassembled proteasome subunits. PLoS Genet. 2015;11: e1005178.
79. Qian SB, McDonough H, Boellmann F, Cyr DM, Patterson C. CHIP-mediated stress recovery by sequential ubiquitination of substrates and Hsp70. Nature. 2006;440:551–5.
80. Ciocca DR, Clark GM, Tandon AK, Fuqua SA, Welch WJ, McGuire WL. Heat shock protein hsp70 in patients with axillary lymph node-negative breast cancer: prognostic implications. J Natl Cancer Inst. 1993;85:570–4.
81. Hwang TS, Han HS, Choi HK, Lee YJ, Kim YJ, Han MY, et al. Differential, stage-dependent expression of Hsp70, Hsp110 and Bcl-2 in colorectal cancer. J Gastroenterol Hepatol. 2003;18:690–700.
82. Tang D, Khaleque MA, Jones EL, Theriault JR, Li C, Wong WH, et al. Expression of heat shock proteins and heat shock protein messenger ribonucleic acid in human prostate carcinoma in vitro and in tumors in vivo. Cell Stress Chaperones. 2005;10:46–58.
83. Conn SJ, Pillman KA, Toubia J, Conn VM, Salmanidis M, Phillips CA, et al. The RNA binding protein quaking regulates formation of circRNAs. Cell. 2015;160:1125–34.
84. Rybak-Wolf A, Stottmeister C, Glazar P, Jens M, Pino N, Giusti S, et al. Circular RNAs in the mammalian brain are highly abundant, conserved, and dynamically expressed. Mol Cell. 2015;58:870–85.
85. Wang R, Zhang S, Chen X, Li N, Li J, Jia R, et al. EIF4A3-induced circular RNA MMP9 (circMMP9) acts as a sponge of miR-124 and promotes glioblastoma multiforme cell tumorigenesis. Mol Cancer. 2018;17:166.
86. Tapescu I, Taschuk F, Pokharel SM, Zginnyk O, Ferretti M, Bailer PF, et al. The RNA helicase DDX39A binds a conserved structure in chikungunya virus RNA to control infection. Mol Cell. 2023;83(4174–89): e7.
87. Wan Y, Hopper AK. Size matters: conserved proteins function in length-dependent nuclear export of circular RNAs. Genes Dev. 2018;32:600–1.

Publisher's Note